NASA Contractor Report 3163

Program for Plasma-Sprayed Self-Lubricating Coatings

G. C. Walther

CONTRACT NAS3-20827
JULY 1979

NASA

NASA Contractor Report 3163

Program for Plasma-Sprayed Self-Lubricating Coatings

G. C. Walther
IIT Research Institute
Chicago, Illinois

Prepared for
Lewis Research Center
under Contract NAS3-20827

National Aeronautics
and Space Administration

**Scientific and Technical
Information Branch**

1979

PREFACE

This is the final report on IIT Research Institute Project D6146, "Program for Plasma-Sprayed Self-Lubricating Coatings," prepared for NASA/Lewis Research Center under Contract No. NAS3-20827. The research work described in this report was conducted during the period November, 1977 to November, 1978. Personnel who have contributed to this work in addition to the author are H.H. Nakamura, W.R. Logan, J.L. Sievert, and Y. Harada.

TABLE OF CONTENTS

SUMMARY

A program to develop a composite powder for plasma-sprayed self-lubricating coatings was pursued. The goals were to improve the compositional uniformity of the sprayed coating and obtain a scheme that could be used by vendor organizations in preparing and applying these powders and coatings. Adhesive strength determinations were made. Both quantitative microscopy and atomic absorption analyses were used to monitor the coating composition distribution.

This study found:

1) suitable composite powders could be prepared by making adjustments to particle size distribution, binder type, and binder concentration.

2) the adhesive strength of the plasma-sprayed coatings increased approximately 40%, from 830 to 1160 psi, following a 20 hour/649^{o}C heat treatment.

3) quantitative microscopy can be used to characterize the composition of the multi-phase plasma-sprayed coating.

4) although the level of CaF_2 was close to or within specification (55$\pm$5 vol %), the amounts of Ag and nichrome desired were essentially reversed; this is attributed to relative loss of nichrome: it is assumed some of refractory nichrome particles solidified and tended to bounce off the substrate and coating while the lower melting Ag particle did not and tended to show a "spat" pattern as molten Ag struck the surface.

5) there was poor agreement between quantitative microscopy and atomic absorption analyses used for determining compositional variability: more work is needed to determine an appropriate quality control measurement method and resolve the observed discrepancies

1.0 INTRODUCTION

The objective of this program was to develop the processing technology necessary to achieve reproducible, high quality plasma-sprayed coatings of uniform composition that have self-lubricating properties over a wide temperature spectrum. This process should be appropriate for commercial production of coatings that have shown promise in experimental laboratory tests.

Quality was to be judged on the basis of reproducibility and uniformity of chemical composition, microstructure, and adhesive strength. To that end it was specified the coating composition variation be within a few percent for two distinct batches prepared separately and plasma-sprayed on three-2" x 2" substrates of Inconel 750 or other nickel based alloy. The coating-substrate adhesive strength must also show less than 50% decrease after a 20 hour heat treatment at 649°C. Wear tests to be performed at NASA/Lewis will determine the self-lubricating characteristics of coatings prepared using the processing described below.

1.1 Technical Background

Plasma-sprayed coatings which are self-lubricating from cryogenic temperatures to 840°C (1600°F) have been developed at NASA/Lewis. Although several solid lubricating materials such as MoS_2, CF_x, and SiO-PbO, give good lubricating properties up to 600°C, the discovery of CaF_2-BaF_2 lubricant mixtures has pushed this operating temperature to 800-900°C. Further developments have improved substrate oxidation resistance by use of suitable glass additions, and extended useful performance to cryogenic

temperature by additions of Ag. Methods of fabricating lubricant coatings by impregnating powder metal structures and by plasma spraying have been achieved.[1,2,3]

One of these coating compositions is designated NASA-LUBE PS106. PS106 is a specific example of coatings covered under U.S. Patent 3953343, "Bearing Materials," assigned to the U.S. Government.[4] PS106 contains three components: silver, nichrome, and calcium fluoride. The rationale of this development is that silver provides lubrication at low temperatures, nichrome improves machinability and thermal matching with typical substrate materials, and calcium fluoride provides high temperature lubrication.

The problem that still remained for the realization of an acceptable commerical application of this material was achieving reproducible coatings for PS106 and related compositions that have predictable and satisfactory cohesive strength, substrate bonding, and lubricating properties. When this is done, the anticipated applications include airframe and spacecraft bearings subjected to re-entry heat and vacuum conditions, as well as applications in liquid metal pumps and heat engine environments.

1.2 Approach To The Problem

IITRI believed the coating variability of concern to NASA was due primarily to changes in the component feed powder characteristics during its preparation, mixing, and introduction into the plasma, and not to parameters which influenced the plasma behavior or spraying operation per se, since the state-of-the-art of plasma-spraying is well established. It has been recognized [5]

that mixing, handling and storage of powders can result in particle segration and aggregation due to size distributions that permit settling. This effect can be even more pronounced when particle density varies greatly, as in the case of PS106 (e.g., Ag = 10.5 g/cm^3 and CaF_2 = 3.2 g/cm^3). During the processing of composite multi-density plasma-spray powders, it is quite possible such segration and non-uniformity of composition occurs. Mixing, feed hopper delivery, gas carrier powder propulsion, and plasma gas turbulence, all have potential for separating powder mixtures from the desired average composition. Improvements in plasma spraying equipment design have reduced these problems, but the main effort there has been directed to using finer powders (of comparable density) for denser coatings.

Therefore, the problem was viewed as one of powder processing and handling, and this is where the program described in the following sections had its major focus. It appeared feasible to reduce segration of such powders by using variations in particle size or by use of suitable binders. Mixtures of particle sizes promotes agglomeration and small particles may adhere to larger ones, creating a pseudo-composite particle. Such a "particle" might remain essentially intact during the plasma spraying process. Alternately, binders could be use to improve the between particle strength of such particle aggregations. The object is then to introduce sufficient binder to the particle connecting necks to achieve maximum strength.

2.0 EXPERIMENTAL PROGRAM

This section describes the characterization, powder processing, plasma-spraying, and strength testing tasks performed during the reporting period. Once the preferred preparation method was determined, wear test samples were also prepared for shipment to NASA/Lewis, as indicated in the last subsection.

2.1 Powder Preparation and Characterization

This section describes the characterization procedures for both starting and spray powders and the preparation method for the latter.

2.1.1 Starting Powder Characterization

The starting powders were obtained from commercial suppliers, as indicated below:

Ag powder	Cerac, Inc. (#1479) -200, +325 mesh
Nichrome powder	Cerac, Inc. (#1572) -150, +325 mesh
CaF_2 powder	Cerac, Inc. (#1570) -150. +325 mesh
CaF_2 powder	Cerac, Inc. (#1462) -325 mesh, 97.7%
CaF_2 powder	Fisher Scientific Co. (#C-89)

The as-received powders were analyzed by x-ray diffraction to ensure their phase content and impurity levels were as specified. Particle size analyses were performed using conventional seiving per ASTM B214 and also a Leeds and Northrop Microtrack Analyzer. This latter instrument circulates a water-powder suspension past a laser light source and detector. Changes in the detected signal

may be converted to a relative particle volume distribution.[6,7] These powders were also examined using binocular optical and scanning electron (SEM) microscopes.

2.1.2 Spray Powder Preparation

The desired composition for PS106, the specified range in composition, and selected physical properties of the component materials are shown in Table 1.

TABLE 1

PS106 COATING COMPOSITION AND PROPERTIES

Material	Wt.%	Vol.%	Density gm/cm^3	Melting Point ^oC
Ag	35±3	20±2	10.5	960
80 Ni-20Cr	35±3	25±2	8.36	1390
CaF_2	30±3	55±5	3.18	1360

Using this basic composition it was proposed the powder mixture's physcial character be modified following the scheme shown in Table 2 to improve coating uniformity and reproducibility. Work at IITRI[8,9] has shown that polyvinyl alcohol (PVA) is a good organic binder, while monoaluminum phosphate (MAP) is a good inorganic binder. The strength of MAP increases significantly following a suitable curing heat treatment. The PVA binder used in this study was Dupont "Elvanol" Grade 51-05, while the MAP binder used was from Mobil Chemical Co.

TABLE 2

PS106 POWDER MODIFICATION MATRIX

Particle Size	Binder	Concentration %
All normal*	None	-
Metal normal-ceramic fine**	None	-
Metal normal-ceramic fine**	Polyvinyl Alcohol	1 and 5
Metal normal-ceramic fine**	Phosphate or Silicate	1 and 5

* Nominally between 100-400 mesh

** Less than 400 mesh

Several trial batches were made using different binder solutions and particle size fractions of CaF_2. The constituent powders were weighed and mixed in the proportions given in Table 1 to make a PS106 powder composition. Mixing was performed in small glass jars which were approximately half full of 1/2" diameter nylon mixing balls. These jars were rotated at ∿100 rpm on a laboratory ball mill for 1 to 1-1/2 hours. Approximately 100 gm quantities were prepared at a time.

Binder solutions of PVA were made by adding tap water to the PVA solid powder and heating at ∿80°C until the solids were dissolved. The MAP binder was already available as a concentrated solution 50-50 by weight and was diluted by adding tap water and stirring.

For those batches prepared using binders, sufficient binder solution was added to the mixed powders to give the desired concentration of binder by weight. This mixture was heated at ∿80-100°C to drive off the water while being continually stirred until dry. This material was ground in a mortar and pestle and then sieved through a 70 mesh screen. This drying step produced hard, brittle nugget, which were difficult to grind. To reduce this problem the drying procedure was changed so that the mixture was only heated until damp and "crumbly". This "crumbly" material was sieved through a 20 mesh screen, dried overnight at 100-115°C, ground to pass a 70 mesh screen, heat treated at 400-450°C for 1-1/2 hours to cure the binder, and then resieved to obtain a -70, +325 mesh powder.

To improve the coating of large particles by finer powder, even smaller particle size CaF_2 was tried next. Attempts were made to obtain finer particles of CaF_2 by ball milling the -325 mesh Cerac CaF_2 powder. Particle size analyses showed this was not productive in a reasonable time using the available laboratory facilities. It was then learned -5 um CaF_2 powder was available from Fisher. This -5μm material was also subjected to particle size analysis and SEM examination.

The final trial batches were prepared by adding approximately half the required CaF_2 powder as -5 μm material. After mixing, adding binder, curing, and sieving, the balance of CaF_2 necessary to make a PS106 composition was added as -150,+325 mesh Cerac CaF_2 powder. Table 3 summarizes the matrix of trial batches produced. Appendix A provides detailed processing information on the final optimized batches as part of a specification sheet.

2.1.3 Spray Powder Characterization

Prior to plasma spraying, powders from selected batches were examined under binocular optical microscope and SEM.

2.2 Plasma Spraying and Coating Characterization

This section describes the set-up and conditions for plasma spraying used in this program. The use of quantitative microscopy, atomic absorption, SEM, and EDX to characterize the coatings is also described.

Table 3

Batch Preparation Details

Batch No.	Amonts of Constituents mixed, gms.					Binder			
	Nichrome	Ag	CaF_2 -150, +325	CaF_2 -325	CaF_2 -5μm	Type	Conc. wt %		
1	35	35	30			--	--		
2	35	35		30		--	--		
3	used for other batches - same as Batch 2								
4	35	35		30		PVA	1		
5	35	35		30		PVA	5		
6	35	35		30		MAP	1		
7	35	35		30		MAP	5		
8	35	35	30			MAP	5		
9	used for other batches - same as Batch 3								
10	35	35		30		MAP	2.5		
11	30	30			15*	MAP	1.25***		
12	30	30	15*, 10.7**			MAP	1.25		
13	30	30	16.2**		15*	MAP	2.5		
14	30	30	15.7**		15*	MAP	6.25		
15	38.5	38.5	13.7**		19.3*	MAP	3.8		
16	38.5	38.5	13.7**		19.3*	MAP	3.8		
17	38.5	38.5	13.7**		19.3*	MAP	3.8		
18	38.5	38.5	13.7**		19.3*	MAP	3.8		
19	38.5	38.5	13.7**		19.3*	MAP	3.8		
20	38.5	38.5	13.7**		19.3*	MAP	3.8		

*added to starting Batch; **added after curing heat treatment; ***became Batch 13 with more binder added.

2.2.1 Set-up

A schematic representation of the plasma spray equipment is shown in Figure 1. Figure 2 shows a view of the Plasmadyne equipment used. A Plasmadyne SG-1-B gun was used for this work. To facilitate spraying the required 2" x 2" areas, a spray-gun holder and traversing carriage were fabricated (see Figures 2 and 3). Powders were fed to the gun from a screw-feed type of powder hopper.

2.2.2 Substrates

Inconel 750 was used for the substrate material. To facilitate subsequent microstructural and compositional analyses, a series of smaller substrates .2" x 375" x 2" separated by .05" spacers to cover the required 2" x 2" area were used. The scheme is shown in Figure 4. The spacers avoid the formation of a "spray-bridge" between samples. This geometry also satisfies NASA's requirements for 0.060" minimum substrate thickness.

An identification number for each 2" x 2" square and an identification letter for each .20" x 2" bar were stamped into one end of each bar, as indicated in Figure 5. The substrates were grit blasted using 20 grit SiC, and cleaned prior to any plasma spraying by brushing with soap and water and a final rinse in acetone.

2.2.3 Actual Plasma Spraying

Batches 15 and 17 were selected for spraying the 2" x 2" squares. Batch 16 was not used because a long interruption during its preparation had occurred. Coatings were sprayed to a thickness of .015-.018". No bond coat was used.

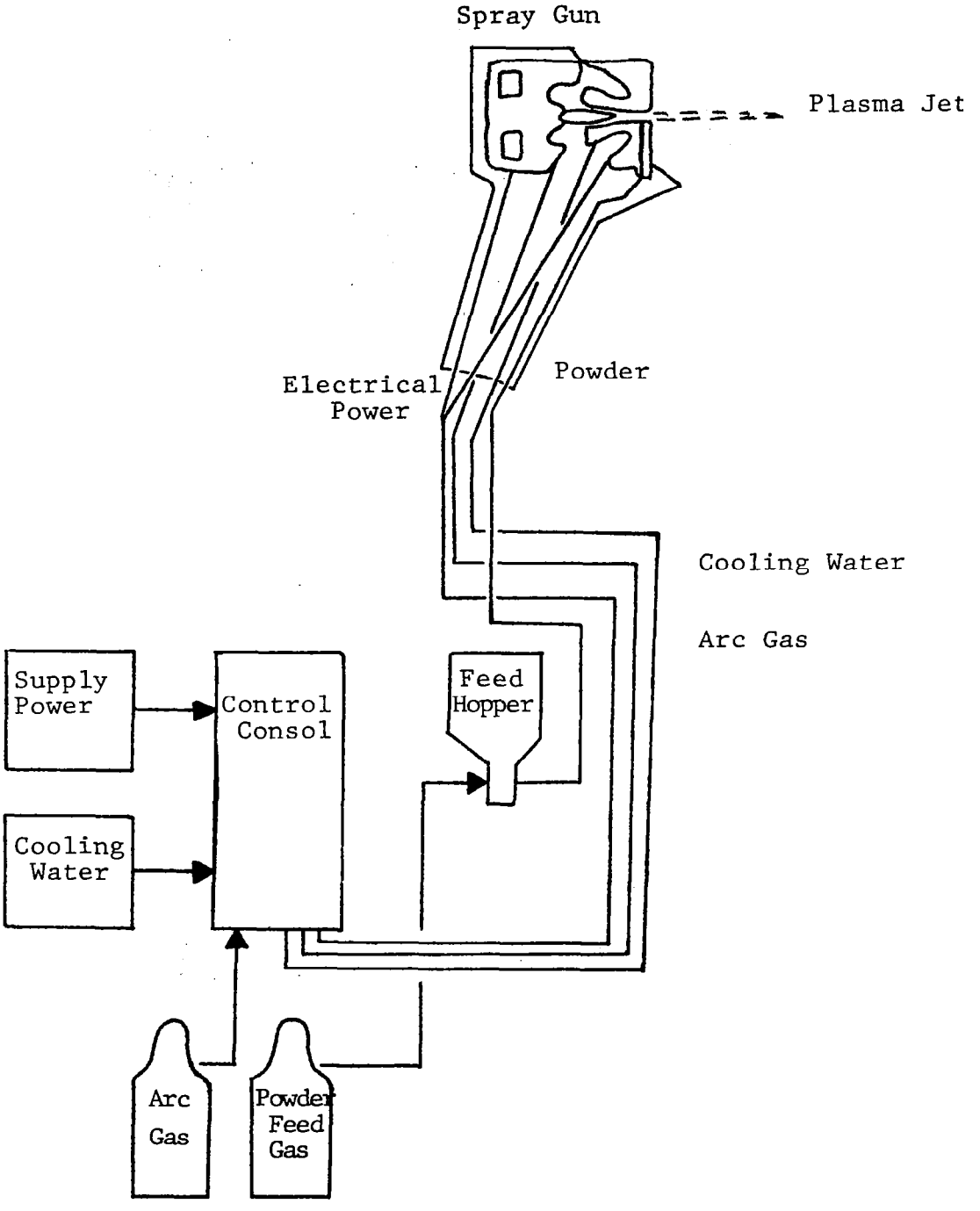

Figure 1 Schematic Representation of the Plasma Spray Process.

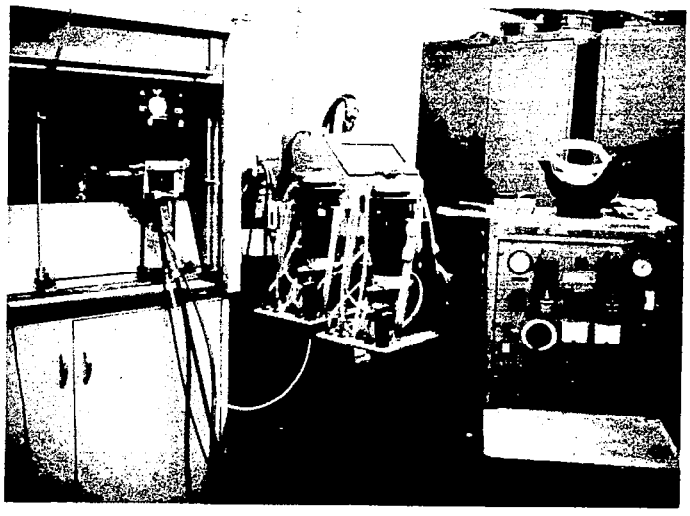

Figure 2 View of the Plasmadyne Equipment.

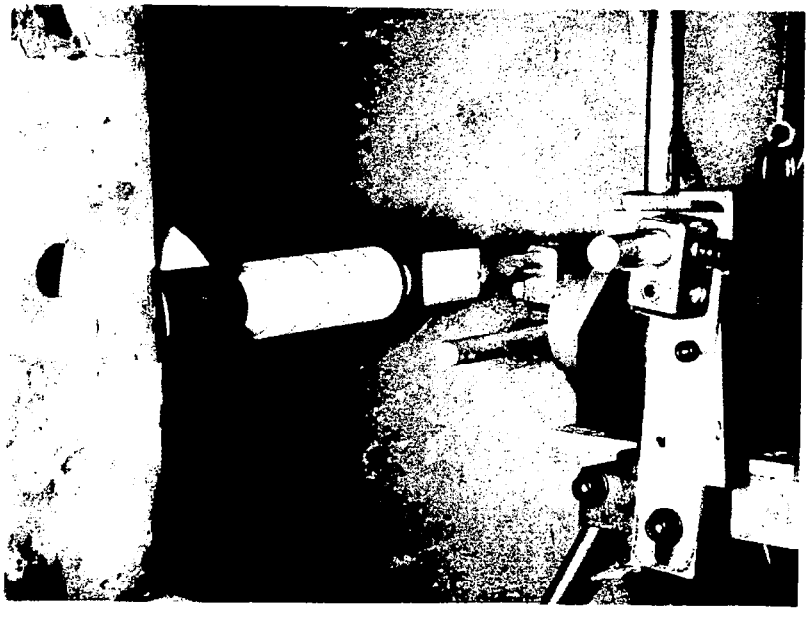

Figure 3 Detail of the spray gun holder.

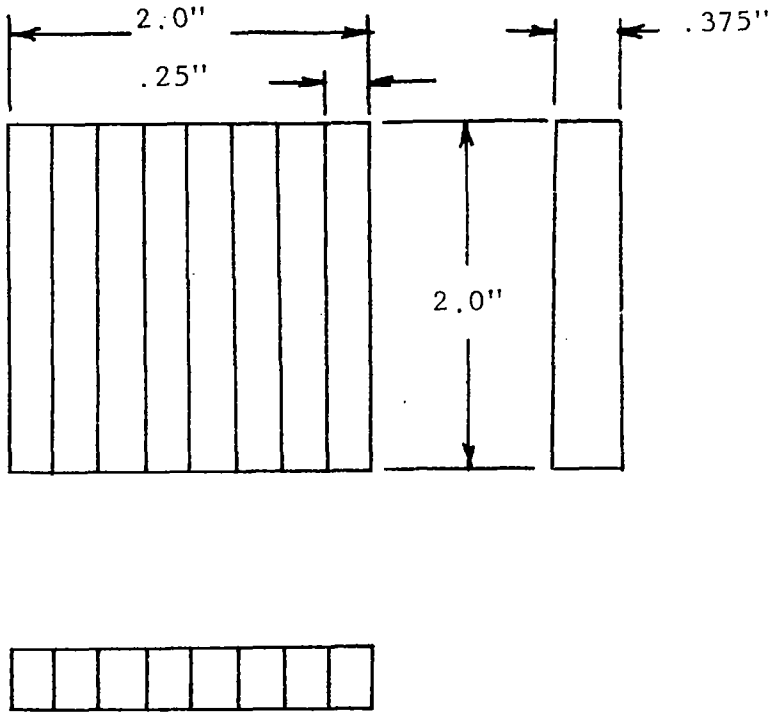

Figure 4. Scheme for plasma-spray substrate.

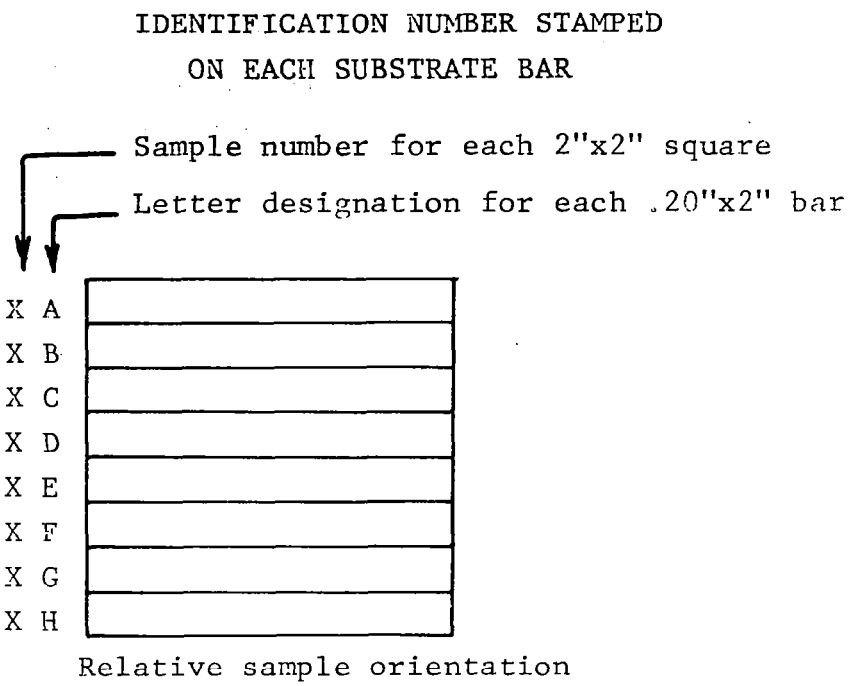

Figure 5 Sample orientation and traversing pattern used during plasma spraying.

Table 4 gives the operating conditions found best for plasma-spraying these powders. Figure 5 shows the relative sample orientation and combined horizontal and vertical traversing pattern used during spraying. Prior to spraying a 2" x 2" substrate, a single horizontal pass was made across a row of microscope slides set at increasing 1/2" intervals from 2" to 5" from the plasma-spray gun. The best coverage on the glass slide was used to set the gun-to-substrate distance for actual spraying.

2.2.4 Quantitative Microscopy Evaluation

Quantative microscopy was used to characterize the degree of compositional uniformity of the plasma-sprayed coatings.[10-14] The basic idea is that geometrical information about a representative three-dimensional structure, such as phase volume, may be obtained from suitable analysis of a representative two-dimensional section through the sample. Such sections are usually prepared metallographically. It can be shown that if a grid is superimposed at several places on such a representative section (as in Figure 6), the volume fraction of the phase of interest (V_V^{Ag}, $V_V^{CaF_2}$, etc.) is equal to the fraction of grid points that fall within the phase

$$V_V = P_P = \frac{\Sigma \text{ \# points within phase of interest}}{(\text{Total \# points in grid})\ (\text{\# of grid placements})}$$

This is true, independent of any assumptions as to phase or particle size and shape and may in principle be applied to analysis of two, five, or twenty phases in the structure. The only limitations are that the structure being examined is sufficiently uniform so that an arbitrarily obtained section will be representative and

Table 4

Operating Conditions for Plasma Spraying

Console Settings

Power - 560 AMPS, 28 Volts

ARC Gas - 65-68 CFH

Powder Gas - 21 CFH

Powder Hopper Setting

Screw Feed - 50 RPM

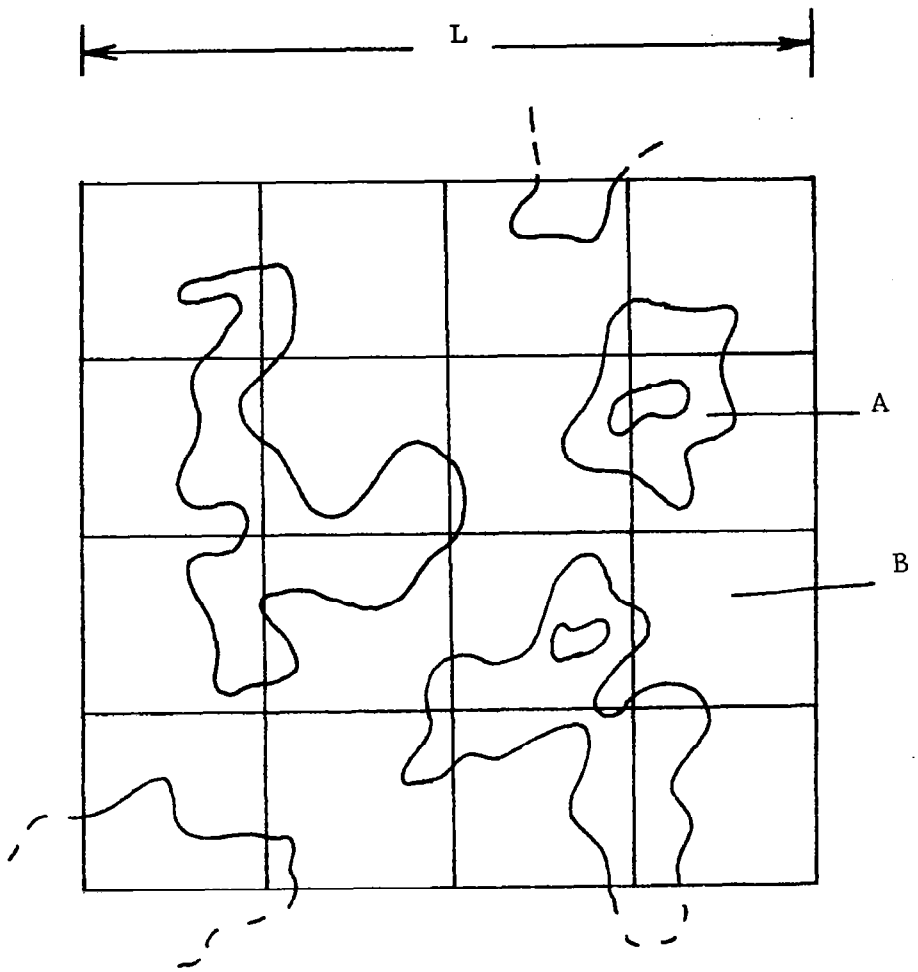

Figure 6 Grid of Length L Placed on a Section Showing Particles of A in a Matrix of B.

that a sufficient number of grid placements be made to get adequate statistical distributions. Twenty-five to fifty placements is usual. The grid can be superimposed in the microscope eye-piece, on photographs, or on a TV screen image.

For this study alternate .20" x 2.0" bars on each 2" x 2" square (letters A,C,E, and G as indicated in Figure 5) were used for evaluation. Each was matallographically polished using 600 grit SiC paper, and then 1000 grit SiC, 10 μm Al_2O_3, and .03 μm Al_2O_3 free abrasive in a nylon polishing cloth. Water was used for a lubricant during polishing.

To delineate the three materials in the polished section, several decoration schemes were examined. Simple electrolytic etches did not appear promising after a few different trials. It was then discovered that a gas phase reaction between H_2S and Ag would create an amber to blue film on the Ag particles while leaving the nichrome phase white and the CaF_2 a translucent gray. It was intended to use this reaction for phase decoration. However, after drying the polished samples overnight at 110°C in a drying oven which contained a dessicant, it was found the Ag phase was already decorated a brown-tan-dark amber and no subsequent decoration treatment was necessary. This assignment of material-color in the polished section was confirmed by SEM-EDX analysis.

The point counting was done manually by superimposing the grid in the microscope eye-piece on the magnified polished sections. There was insufficient gray level contrast of the decorated phases to use the Quantimet Image Analyzing Computer. Figure 7 shows

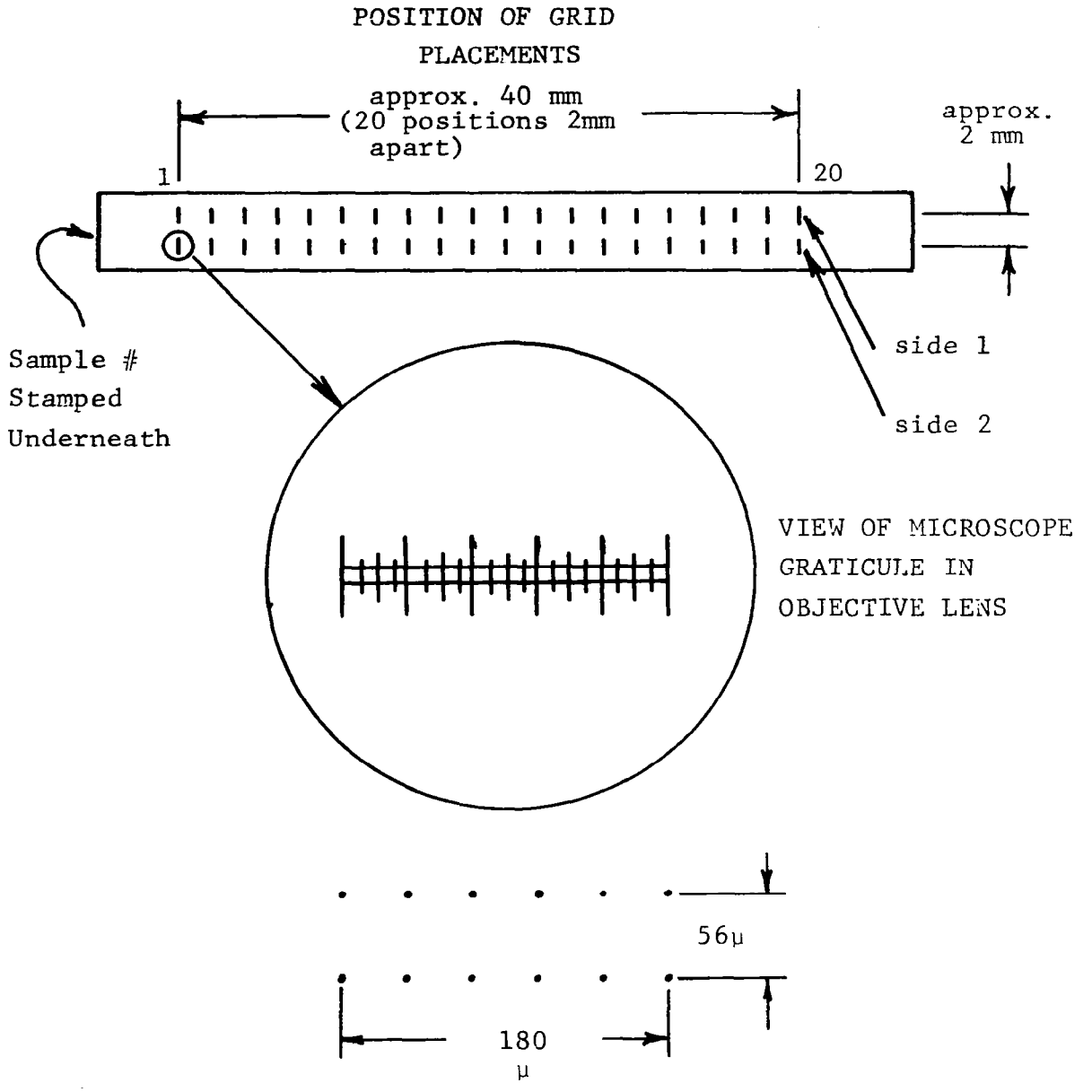

Figure 7 Scheme for making quantitative microscopy measurements.

the general scheme used for these measurements. The grid was superimposed at forty different sites on each .2" x 2" bar examined by moving the sample past the objective lens at 2mm intervals along the bar length. Twenty such grid placements were made on each side of the bar, separated by 2mm to best sample the .2" x 2" area in an efficient manner. Since the available microscope graticule was not a 4 x 4, 5 x 5, or 6 x 6 grid, the ends of the graticule lines were used to establish an equivalent 2 x 6 grid of points with the real distance dimensions shown in Figure 7. These dimensions correspond to the approximate particle size of the microstructural features being examined so they also provide for efficient manual point counting. A total of 480 counts (12 grid points x 40 grid placements) were available for each of the 24 bars examined. The counts were tabulated and the mean and standard deviation of their distribution calculated to provide an indication of the variability within and between each bar.

2.2.5 Atomic Absorption Characterization

One bar from each of the six 2" x 2" squares and a powder mixture of Batches 15 and 17 were used to obtain samples for atomic absorption analysis. These were intended as a check on the quantitative microscopy measurements. These particular bar samples were selected because the quantitative microscopy results for CaF_2 were either right on specification (55 vol. %) or showed significant deviation. The tested pieces were obtained by chiseling off the coating at one end of the bar.

These samples were sent to a commercial laboratory for analysis. Their procedure was to:

1) weigh the desired amount of sample,
2) dissolve it in concentrated HNO_3 acid,
3) heat solution to the boiling point of HNO_3 acid (86°C),
4) bring the solution to a specific volume,
5) measure Ag and Ca weight fractions by atomic absorption.

They indicated there was a slight residue from possible insoluble material in the CaF_2 and/or Nichrome.

2.3 Adhesive Strength Tests

The adhesive strength of sprayed coatings was measured using the procedures specified in ASTM C633. Essentially, a coating was sprayed on a fixture-substrate, machined flat, if necessary, and a second fixture glued to it using a V-block for alignment and an epoxy adhesive. Thus a metal-composite-adhesive metal sandwich results (see Figure 8). This set-up was pulled in tension (Figure 9) until failure occurred and the strength determined from failure load and cross-sectional area. If failure occurs at the bond interface, the bond strength is determined, and if failure occurs within the coating, a measure of cohesive strength may be available. In the latter case the bond strength would be greater than the cohesive strength.

Several samples were joined and tested at room temperature. Several others were joined after the coating-substrate had been exposed to 649°C in air for 20 hours.

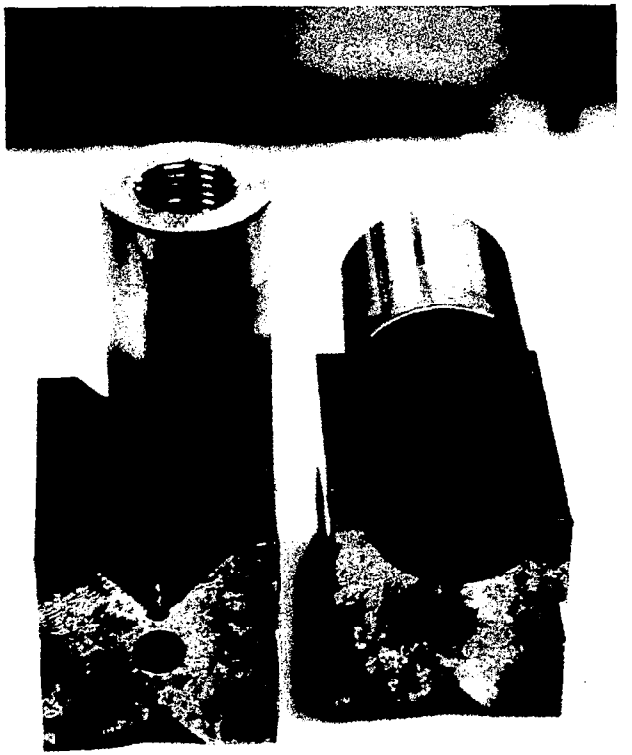

Figure 8 View of Adhesive Strength Samples Prior to Test.

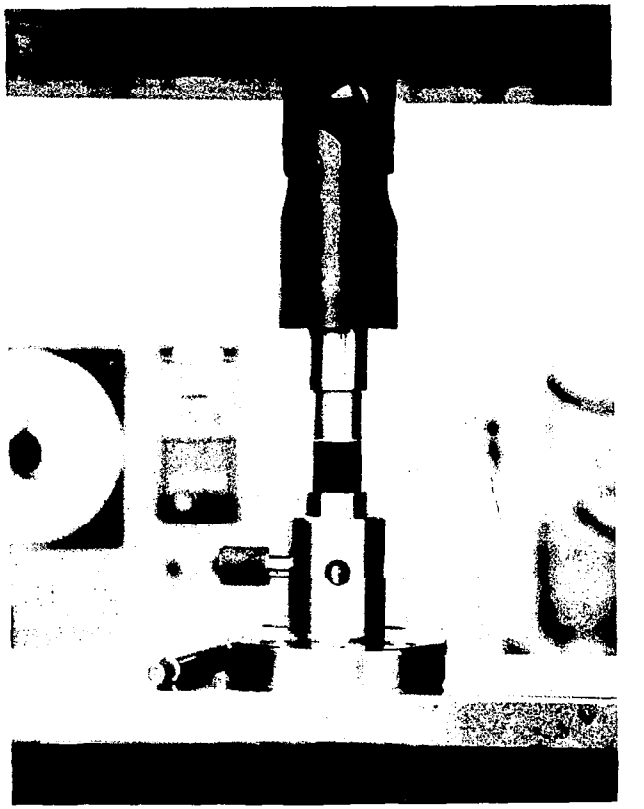

Figure 9 Adhesive strength tension set-up.

2.4 NASA Wear Test Samples

Ten rings and twenty rub blocks were fabricated from Inconel 750 to the configurations indicated in Figures 10 and 11. A .015"$\pm$.003" coating was then plasma sprayed on the outer rim of each ring and the rub surface of each block using the optimised powder preparation-plasma spraying technique. These were sent to NASA/Lewis for wear testing by NASA personnel.

3.0 RESULTS

This section presents the results obtained during the course of this work.

3.1 Starting Powder Characterization

This characterization showed the available powders were suitable for this study. The x-ray diffraction results are tabulated in Table 5. All the powders had the correct phase as expected and no undesired phases were detected (x-ray diffraction typically requires a minumum of 1-5 vol.% be present to be detected). Table 5 also shows peaks are available for quantitative x-ray analysis (i.e. no overlap) should it be required in the future.

The actual particle size range was greater than the nominal size range. Particle size fractions on a weight basis obtained from a sieve analysis are shown in Figure 12. The powders of nominal size -150,+325 mesh (Nichrome and CaF_2) or 200,+325 mesh (Ag) all had a significant fraction of material pass the 325 mesh sieve (11-20% by weight). The Nichrome powder also had $\sim$ 8% retained on the 140 mesh sieve. Almost all of the nominal -325 mesh CaF_2 passed a 400 mesh sieve.

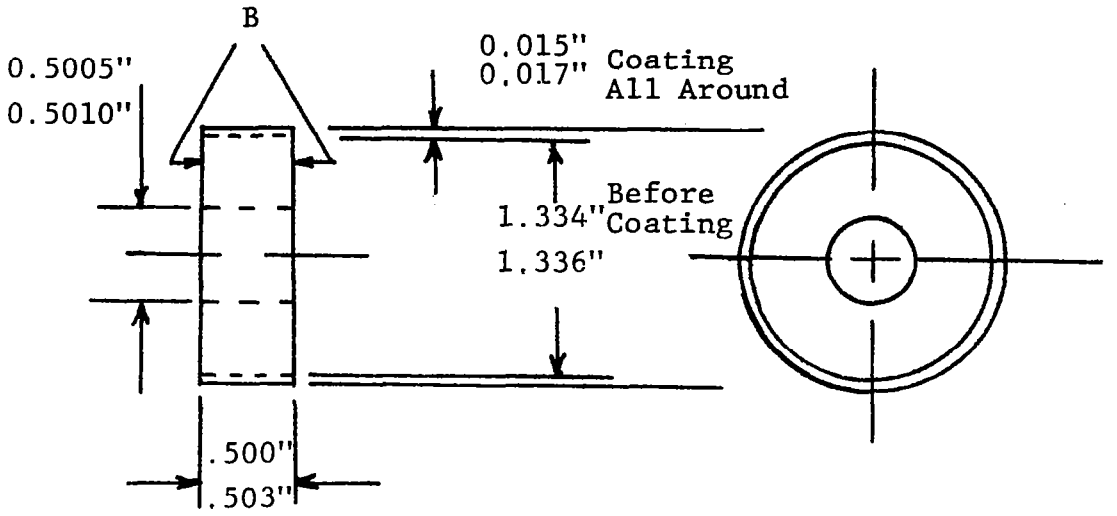

Figure 10 Ring Specimen for NASA Line-Contract Rub Shoe Wear Test Machine

Notes: Both Figures.

1) Bore Diameter to be concentric with O.D. (Before Coating) and square with B surface within 0.001" F.I.R.
2) Break sharp edges on center hole.
3) NASA will machine coatings.
4) 63 maximum all machined surfaces.
5) Sand blast A surfaces before coating.

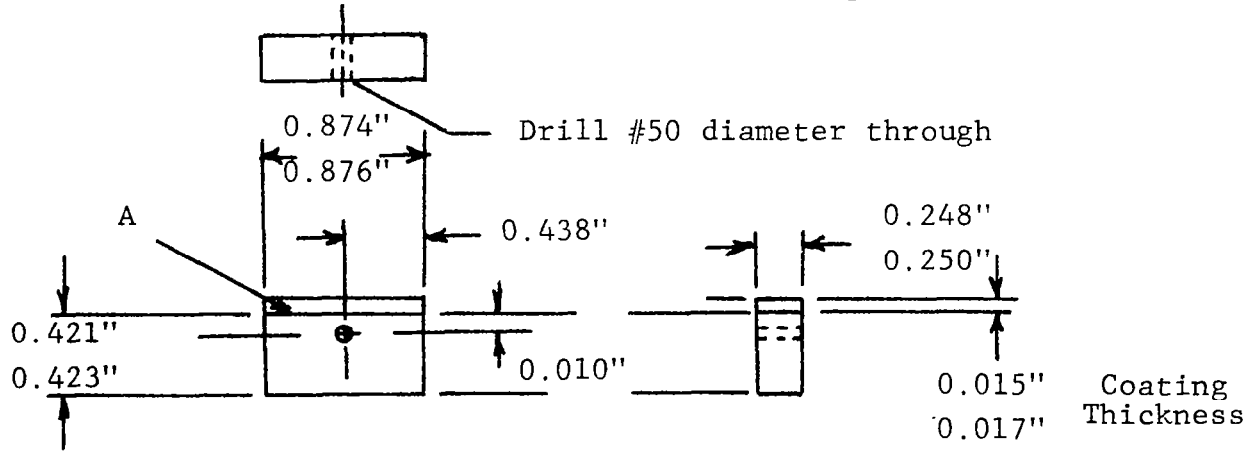

Figure 11 Rub Block Specimen for NASA Wear Test Machine.

TABLE 5

X-ray Patterns For
Plasma Spray Powder Materials

$2\theta^{o}$ Cu Kα	d $\overset{o}{A}$	I/I_i	hkl		$2\theta^{o}$ Cu Kα	d $\overset{o}{A}$	I/I_i	hkl	
SILVER - Ag PATTERN 4-0783					CALCIUM FLUORIDE - CaF_2 PATTERN - 4-0864				
38.15	2.359	100	111	*	28.30	3.153	94	111	*
44.39	2.044	40	200	*	47.06	1.931	100	220	*
64.48	1.445	25	220	*	55.82	1.647	35	311	*
77.55	1.231	26	311	*	68.71	1.366	12	400	*
81.61	1.1796	12	222		75.94	1.253	10	331	*
97.99	1.0215	4	400		87.48	1.1150	16	422	
110.63	0.9375	15	331		94.34	1.0512	7	511	
115.36	0.9137	12	420		105.93	0.9657	5	440	
135.10	0.8341	13	422		113.22	0.9233	7	531	
					115.70	0.9105	1	600	
					126.39	0.8637	9	620	
					135.47	0.8330	3	533	
NICKEL - Ni PATTERN 4-0850					CHROMIUM - Cr PATTERN 6-0694				
44.54	2.034	100	111	*	44.41	2.04	100	110	*
51.89	1.762	42	200	*	64.64	1.4419	16	200	
76.44	1.246	21	220	*	81.80	1.1774	30	211	*
93.04	1.0624	20	311		98.25	1.0195	18	220	
98.55	1.0172	7	222		115.40	0.9120	20	310	
122.09	0.8810	4	400		135.64	0.8325	6	222	
144.95	0.8084	14	331						
156.08	0.7880	15	420						

* Indicates peaks observed.

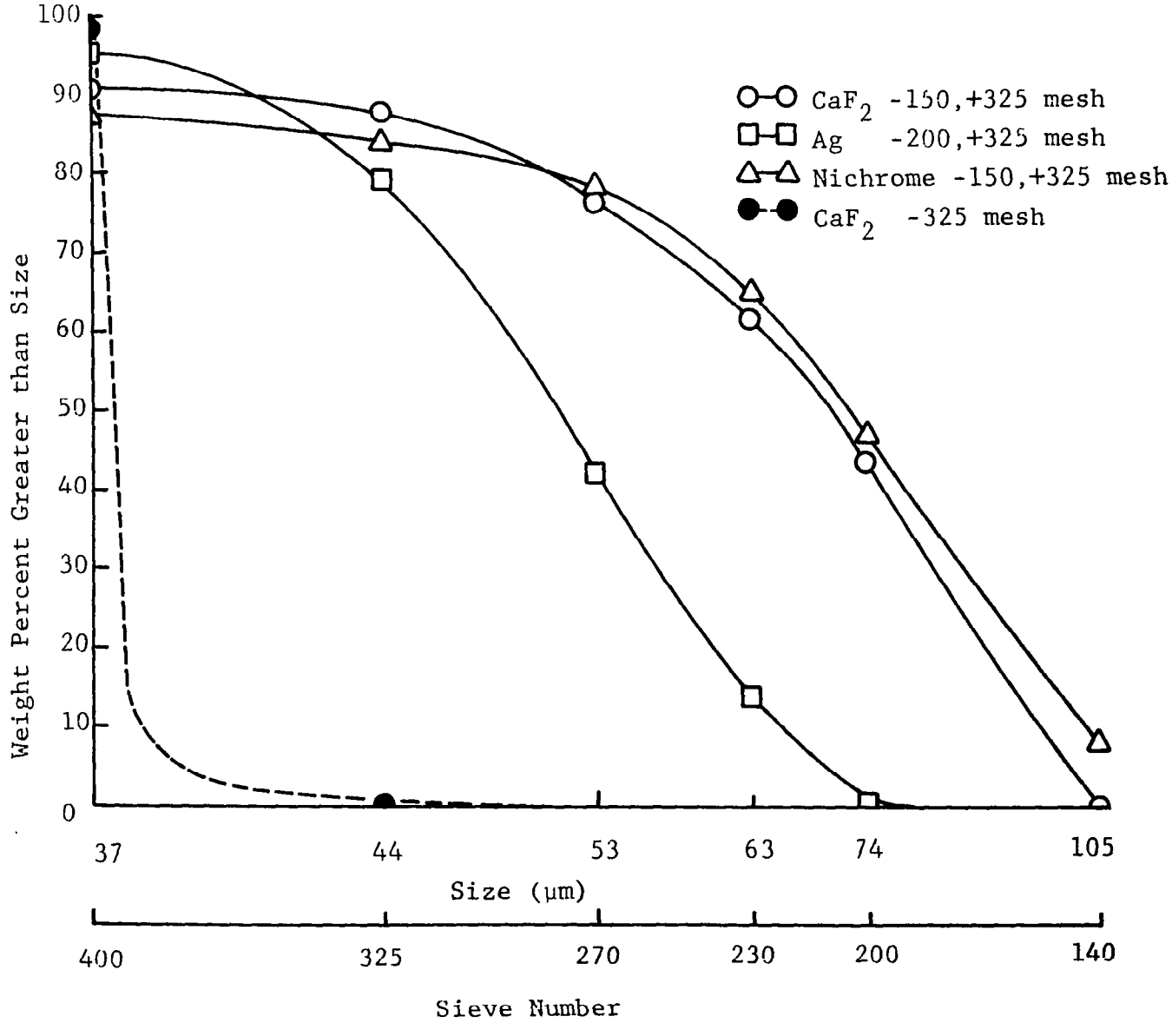

Figure 12 Particle Size Distribution from Sieve Analysis.

The particle size distribution obtained on a volume basis using the Microtrack Analyzer are shown in Figure 13. These results agree with the sieve analyses except they tend to indicate a larger portion of material is larger than specified. The measurements on nominal -5μ powder shows it is almost all less than 20μ and mostly less than 10μ in size.

Observations by optical binocular microscope and SEM of the starting powders and samples from the sieve fractions showed the following:

1) The as-received commercial nichrome powder was a mixture of spherical globules and rougher, elongated agglomerates of smaller globules. These globule particles had a dull metallic coloring. Figure 14 shows an SEM micrograph of this material.

2) The Ag powder was made up of angular, faceted, equiaxed grains although a few spherical globules and agglomerated particles were observed. These particles had the bright, shiny appearance expected for Ag. Figure 15 shows an SEM micrograph of the Ag powder.

3) The characteristics observed for the CaF_2 powder varied with particle size. Most particles were clear although some were milky colored globules, with some brown-red, amber, and purple grains also observed. The larger particles were usually equiaxed but as the particle size decreased many more grains shown pronounced elongated character, with "length to diameter" ratios of $\sim$ 3. This material was angular and rough (see Figure 16). The nominal -325

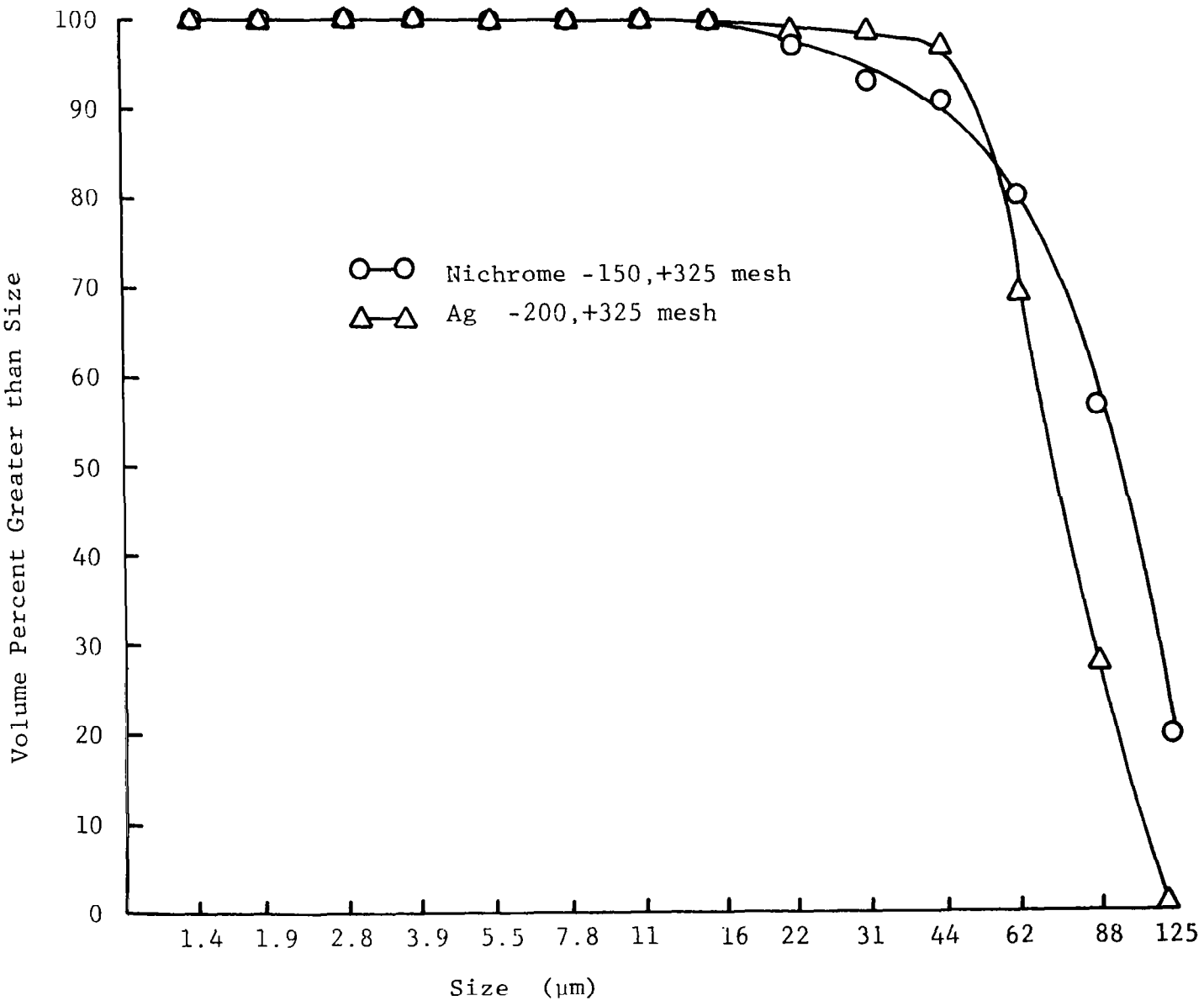

Figure 13 Particle Size Distribution from Microtrack Analyzer.

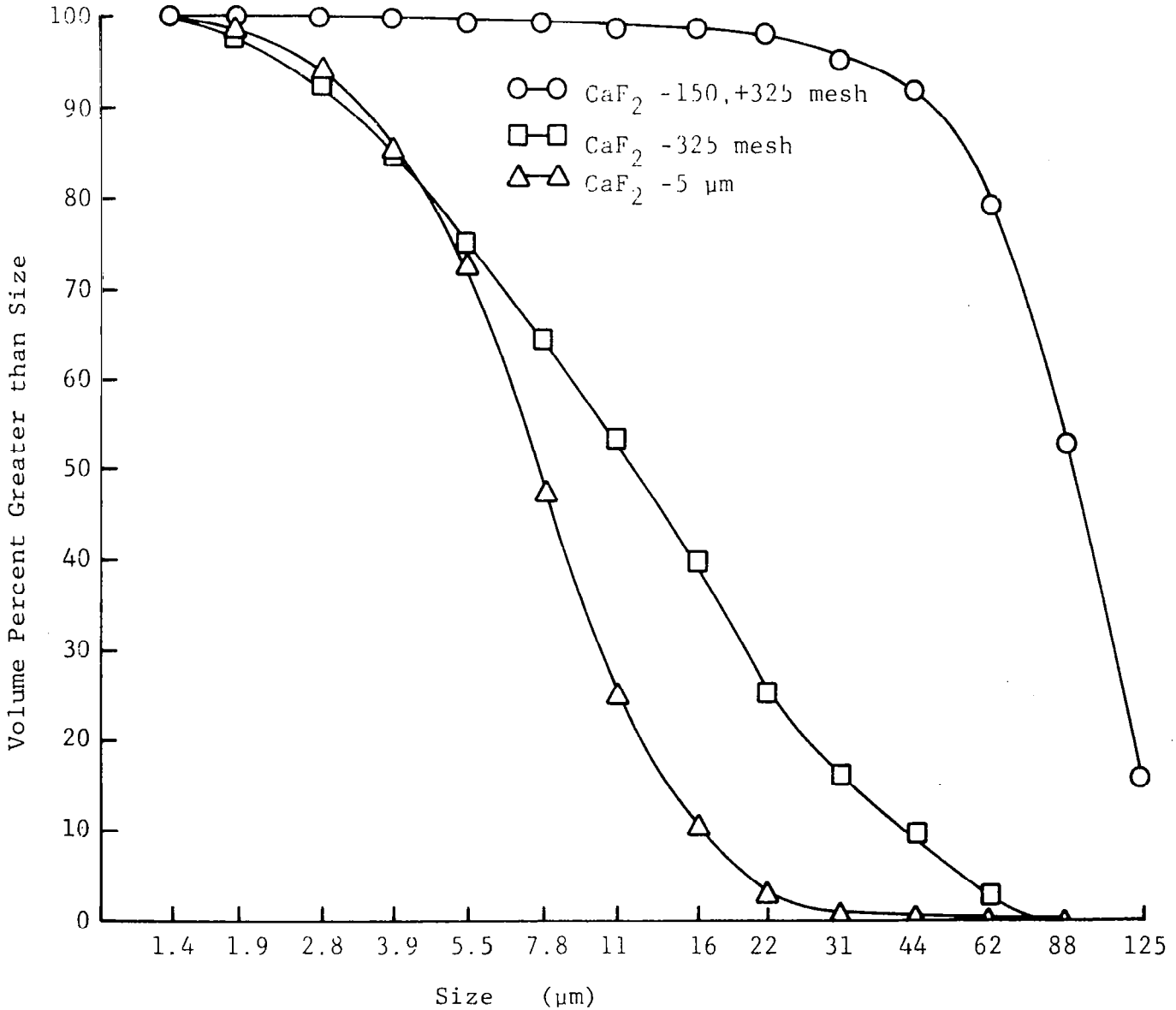

Figure 13. Concluded.

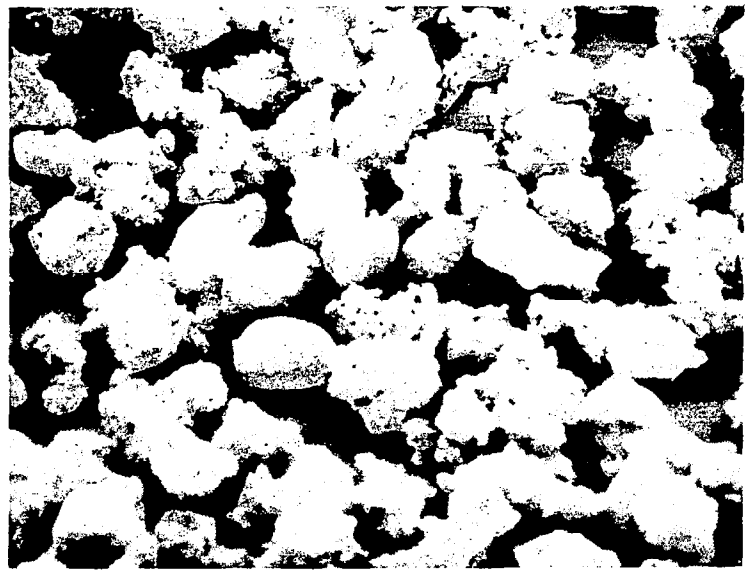

-140,+200 mesh sieve fraction (100X)

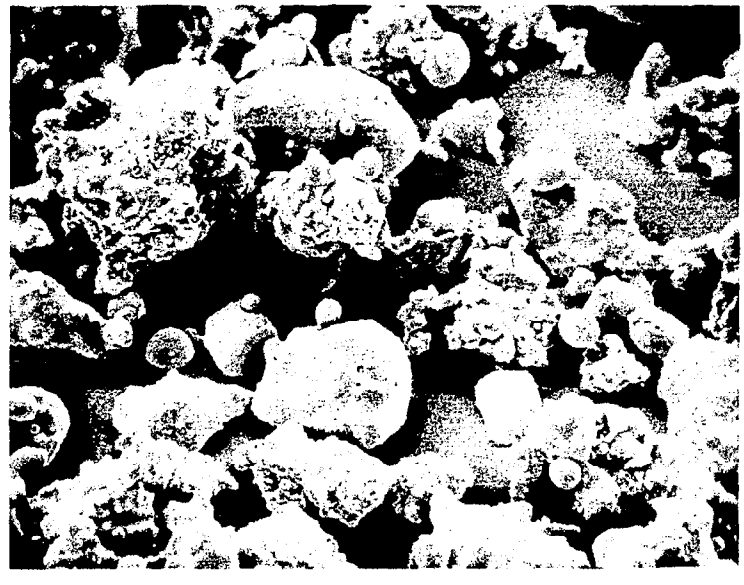

-400 mesh sieve fraction (500X)

Figure 14 Starting Nichrome Powder.

-230,+270 mesh sieve fraction (200X)

-400 mesh sieve fraction (200X)

Figure 15 Starting Ag Powder.

-140,+200 mesh sieve fraction (100X)

-400 mesh sieve fraction (200X)

Figure 16 Starting -150,+325 mesh CaF_2 powder.

mesh CaF_2 also showed a bimodel particle size distribution, some particles in the 20-30 μ range and a much finer size fraction around 1 μ (Figure 17). The Fisher -5μ CaF_2 powder showed similar characteristics except it tended to be more equiaxed (Figure 18).

3.2 Characterization of Batch Powders

The characterization of batch powders prior to spraying consisted of binocular optical microscope and SEM observations and observed behavior of these powders during their preparation. Batches 1 and 2, made without binders, showed no real agglomeration. Batches 4 and 5, made with 1 wt % and 5 wt % PVA binder, respectively, did show some agglomeration, but their mixing and grinding behavior was judged unsatisfactory in that larger nuggets were retained during the heating to dryness step in their preparation. This required excessive grinding, which created more fines than desired (see Figure 19). Batch 6, using 1 wt % MAP binder and -325 mesh CaF_2 showed some agglomeration but also excessive powdering from the grinding step, suggesting not enough binder was added (Figure 20). Adding up to 5 wt % MAP (Batches 7 and 10) reduced the powdering somewhat but still did not form the desired agglomerates (see Figure 21). Adding 5 wt % MAP to powder containing -150,+325 mesh CaF_2 (Batch 8) created good composite agglomerates but this was an excessive quantity of binder for the smaller particle surface area using the larger CaF_2 particles (Figure 22).

Next the use of -5μm CaF_2 with MAP binder was examined. For Batch 11 it was intended to add the CaF_2 in two stages: first use -5μm CaF_2 with 1.25% binder and add the balance of needed CaF_2

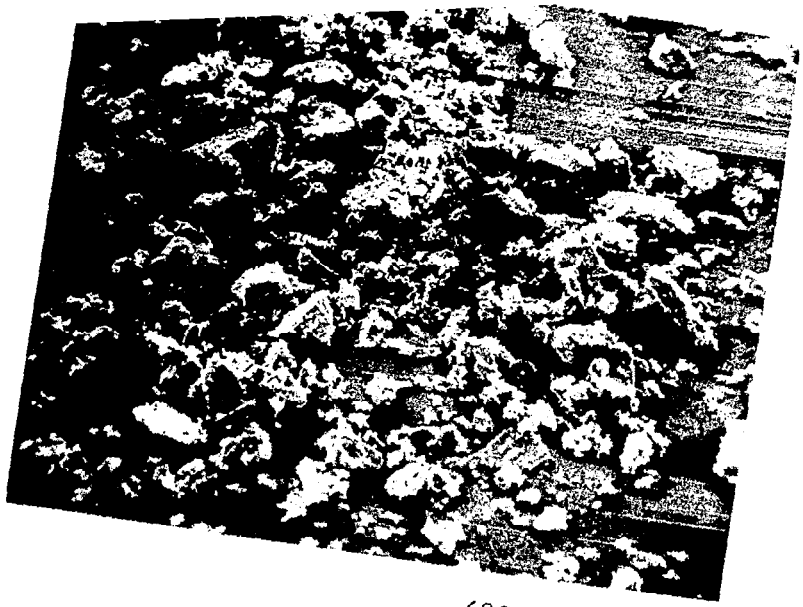

(200X)

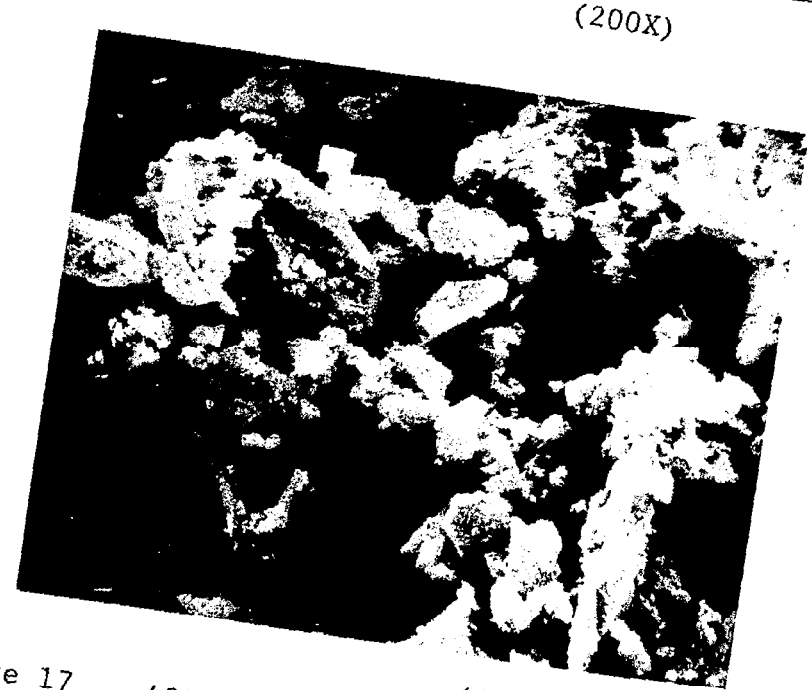

(2000X)

Figure 17 -400 mesh portion of the -325 mesh Cerac CaF_2 powder, showing the bimodel size distribution.

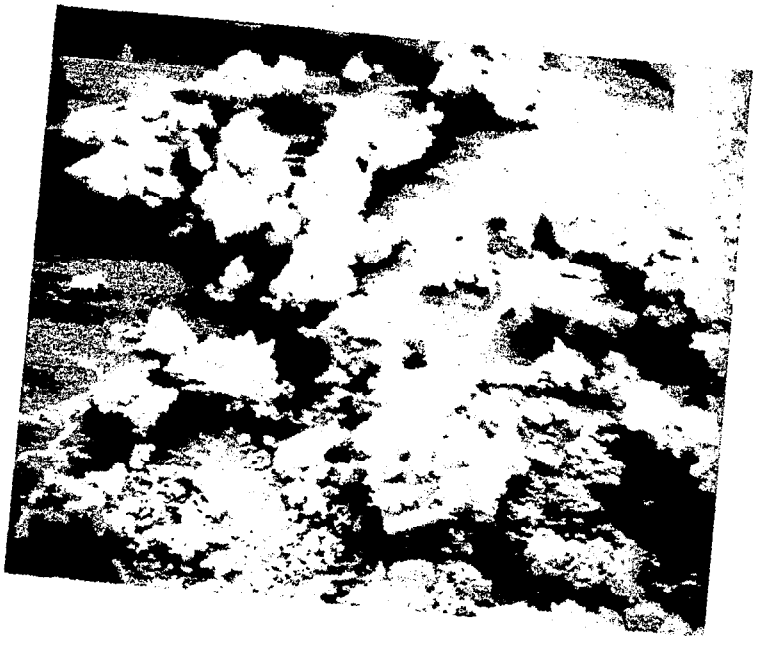

Figure 18 Fisher -5 μm CaF_2 powder (1500X).

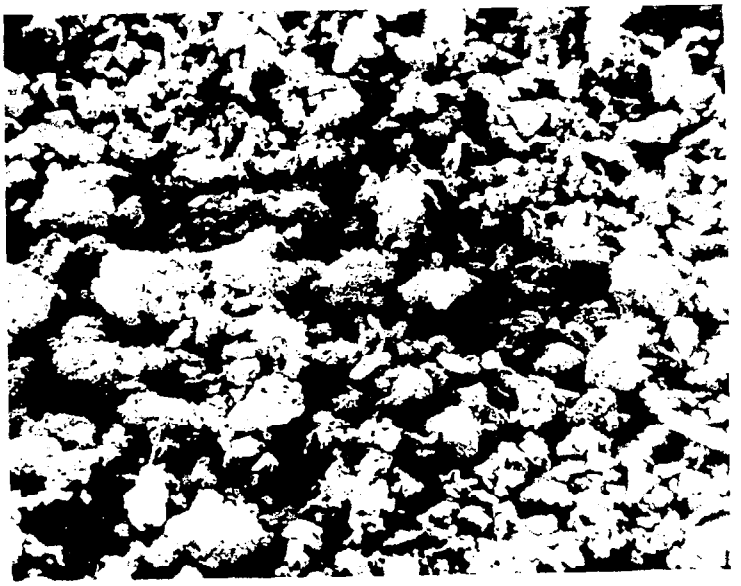

Figure 19 Batch 4 powder made with 1 wt% PVA binder and -325 mesh CaF_2 powder (100X).

Figure 20 Batch 6 powder made with 1 wt% MAP binder and -325 mesh CaF_2 powder (50X).

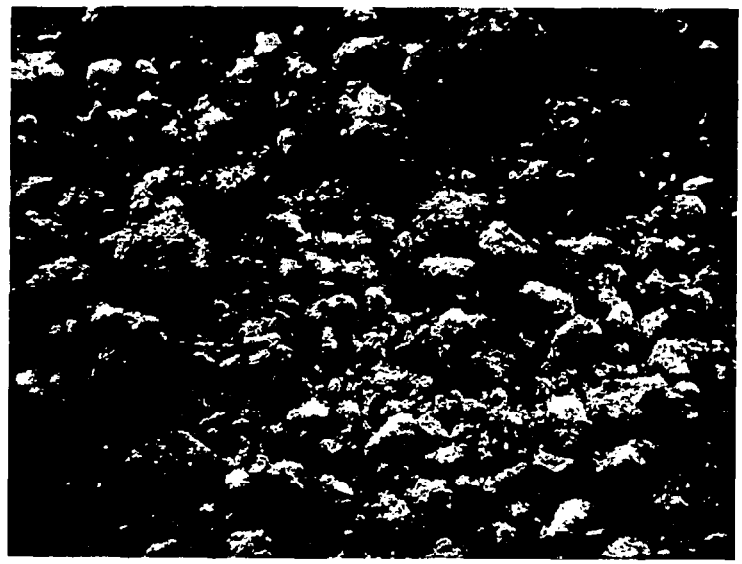

Figure 21 Batch 7 powder made with 5 wt% MAP binder and -325 mesh CaF_2 powder (50X).

(50X)

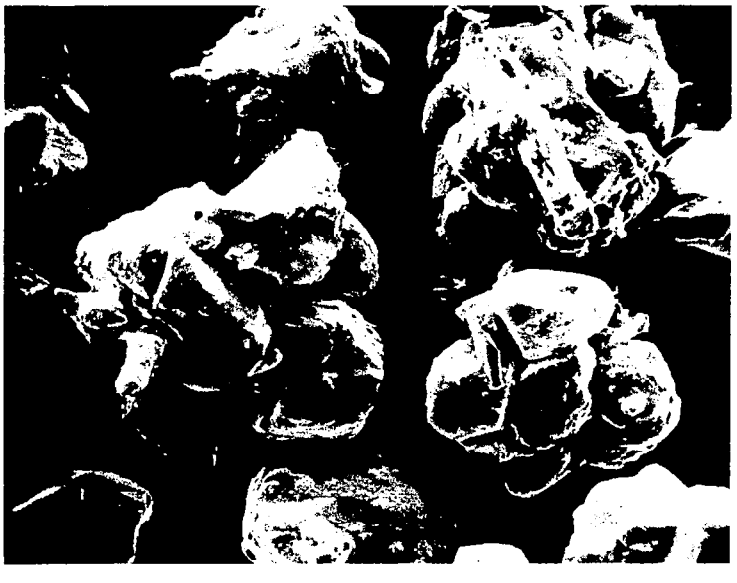

(200X)

Figure 22 Batch 8 powder made with 5 wt% MAP binder and -150,+325 mesh CaF_2 powder.

as -150,+325 mesh material. This proved to be an inadequate quantity of binder so more was added and this batch was designated Batch 13. Batch 12 also used the concept of adding CaF_2 in two steps, but -150,+325 mesh material was used for both additions. Figure 23 shows it did not form agglomerates as desired. Batches 13 and 14 both used an initial level of -5μm CaF_2 with -150,+325 mesh material added later and 2.5 and 6.25 wt % MAP, respectively. Batch 13 showed good agglomeration with some small levels of powdering (Figure 24), while Batch 14 appeared to have formed more agglomerates of -5μm CaF_2 than forming CaF_2 -Nichrome-Ag composite particles (Figure 25).

In conjunction with the initial plasma spray results, Batch 13 appeared to be the best except for a little powdering during grinding and sieving. It was decided to increase the binder concentration to 3.8 wt % for the samples plasma-sprayed to demonstrate compositional uniformity and adhesive strength, and for the NASA wear tests. Thus Batches 15 through 20 were made using both -5μmCaF_2 and 150,+325 mesh CaF_2 with 3.8 wt % MAP binder. Figure 26 shows powder from a mix of Batches 15 and 17. Although not evident in the black and white photographs of Figures 24 or 26, under the optical microscope the composite particles of Batches 13 and 15 + 17 could be seen as few large metal particles with a packing of fine white powder around them. Thus the goal of preparing suitable composite "particles" was achieved.

Figure 23 Batch 12 powder made with -150,+325 mesh CaF_2 powder and 1.25 wt% MAP binder (160X).

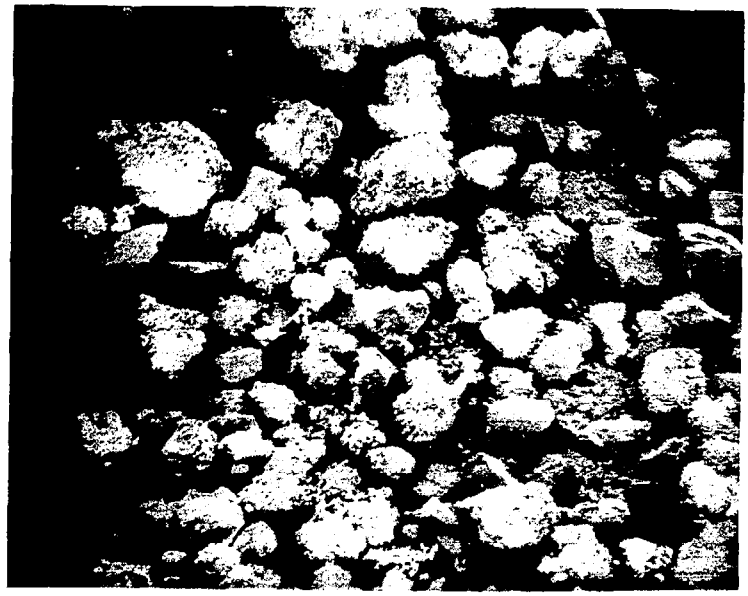

Figure 24 Batch 13 powder made with -5 μm CaF_2 and -150,+325 mesh CaF_2 powders and 2.5 wt% MAP binder (80X).

Figure 25 Batch 14 powder made with 6.25 wt% MAP binder and -5 μm and -150,+325 mesh CaF_2 powder (80X).

(400X)

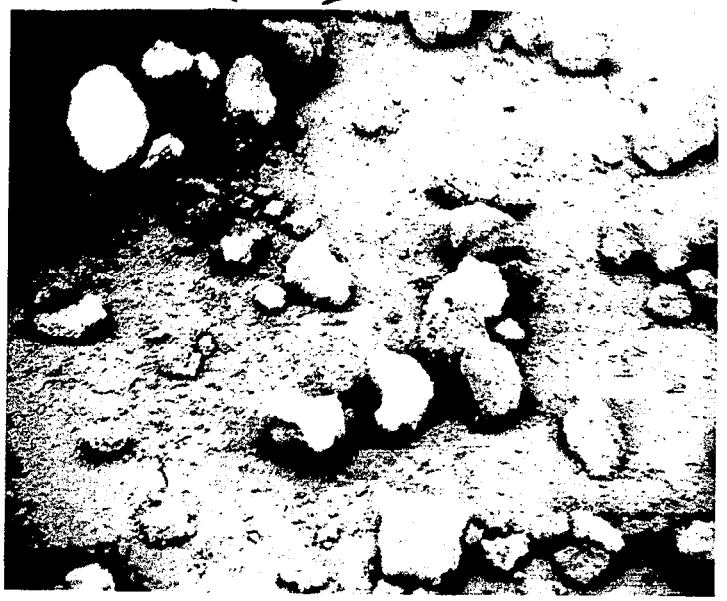

(40X)

Figure 26 Batch 15+17 powder made with -5 μm and -150,+325 mesh CaF_2 powders and 3.8 wt% MAP binder.

3.3 Characterization of Plasma Sprayed Coatings

The plasma-sprayed coatings were examined visually, by using a binocular optical microscope, by SEM-EDX analysis, by quantitative microscopy, and by atomic absorption measurements.

3.3.1 Visual and Microstructural Observations

The as-plasma-sprayed appearance of the substrates sprayed with Batches 10-13 is shown in Figure 27. Batch 10 is darker than the other three and slight color variations are visible in each, although the Batch 13 result looks the most uniform. The coating appeared tan with some darker red-brown coloration, which is presumably a silver oxide. Figure 28 shows the appearance of the six substrates used for checking compositional uniformity. There is still some color variation but in general they are pretty uniform. Brushing these surfaces with a stiff bristle brush removed the brown coloration and no obvious variation was then visible. Figure 29 shows a similar view of the as-sprayed NASA wear test ring samples.

As indicated above, the samples were polished and decorated in preparation for quantitative microstructural analysis. The result was that the nichrome phase appeared white, the Ag appeared light brown, and the CaF_2 appeared grey or translucent when viewed in the metallographic microscope. This phase color assignment was confirmed by SEM examination and by energy dispersive x-ray analysis (EDX), as indicated below. An SEM micrograph of a typical polished section is shown in Figure 30. (The grey shade coloration is different in the micrograph from that given for optical observations). In general, the nichrome phase is

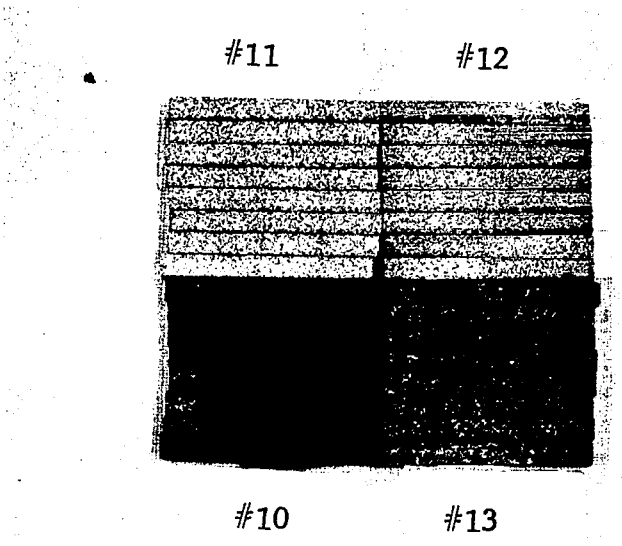

Figure 27 As plasma-sprayed appearance of substrates sprayed with Batches 10-13.

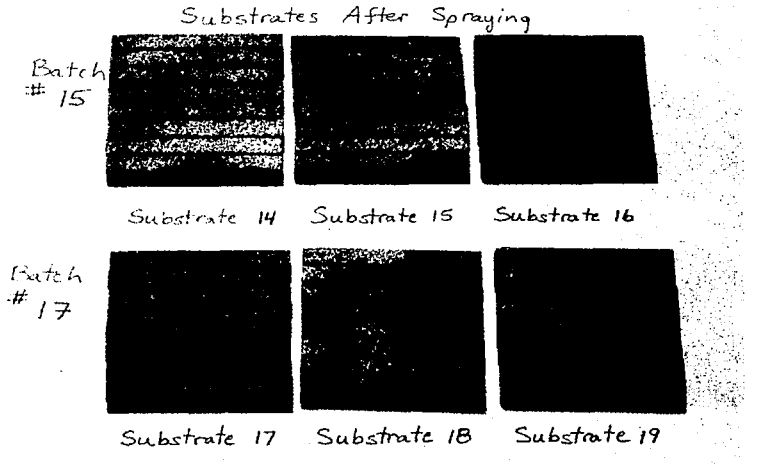

Figure 28 As plasma-sprayed appearance of the six substrates used for checking compositional uniformity.

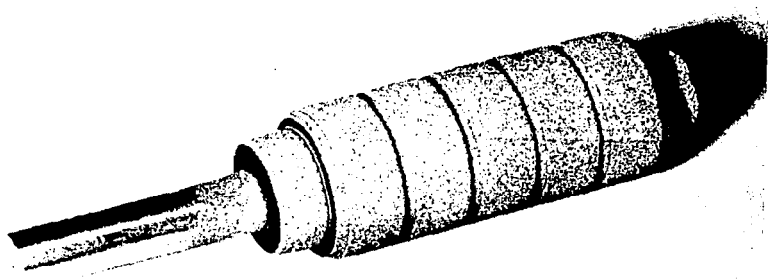

Figure 29 As-sprayed appearance of the NASA wear test ring samples.

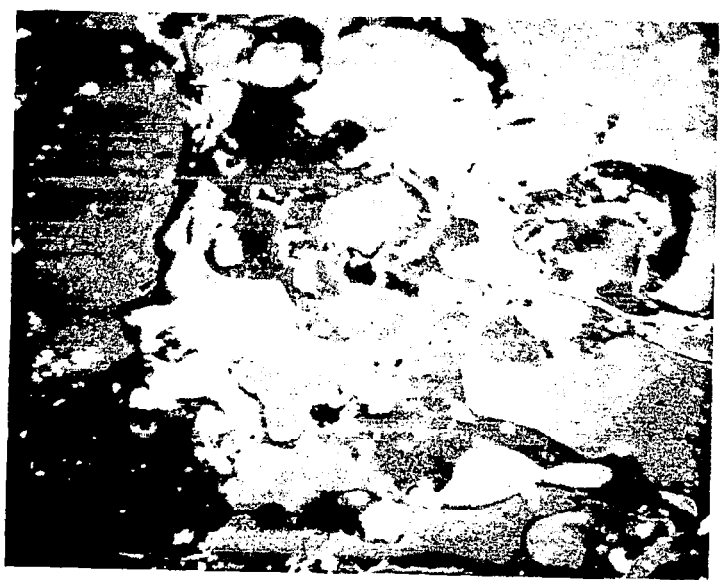

Dark = CaF_2

Light= Ag

Gray = Nichrome

White particles are artifact

Figure 30 SEM micrograph of a typical polished section (500X).

more circular, indicating more equiaxed particles in three dimensions. In contrast, the Ag phase appear more serpentine, suggesting more spattering and spraying of the soft or molten Ag particles upon impact with the substrate. This is further confirmed by observations of the sprayed glass slides used to established gun-substrate distance.

Some porosity is evident, estimated to be less than 3% by volume. Some of the observed porosity may be due to particle "pull-out" during metallographic preparation, especially of the brittle CaF_2 ceramic.

The EDX analysis is indicated in Figure 31. Higher magnification views in Figure 32 show polishing scratches on the nichrome particles and a series of small stippled holes from the oxidation reaction on the Ag particle, identical to that seen in the metallographic microscope. These further confirm the phase color assignment given above. The white particles seen on the polished surfaces are an artifact. EDX shows they contain Ca and P. They may be from the dessicant in the drying over or from CaF_2 particles fractured during the process of chiseling SEM samples off the substrate.

After the initial batches were prepared and plasma-sprayed, these samples were polished and examined using a binocular optical microscope. It was necessary to adjust the angle of illumination to best see the nature of the polished surface since the clear and translucent CaF_2 particles tended to be seen as "extra" porosity unless viewed properly. These observations showed Batch 13 had

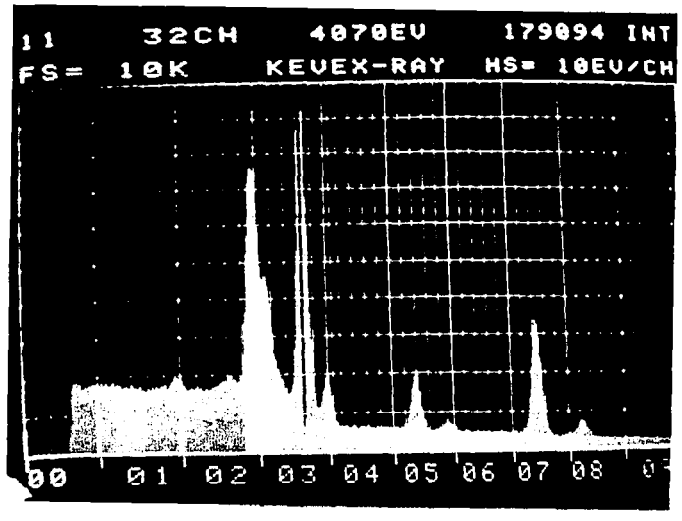

2.0 = P
2.6 = Cl
2.9 = Ag
3.1 = Ag
3.7 = Ca
4.0 = Ca
5.4 = Cr
5.9 = Cr
7.5 = Ni
8.3 = Ni

EDX scan showing energy window for Ag

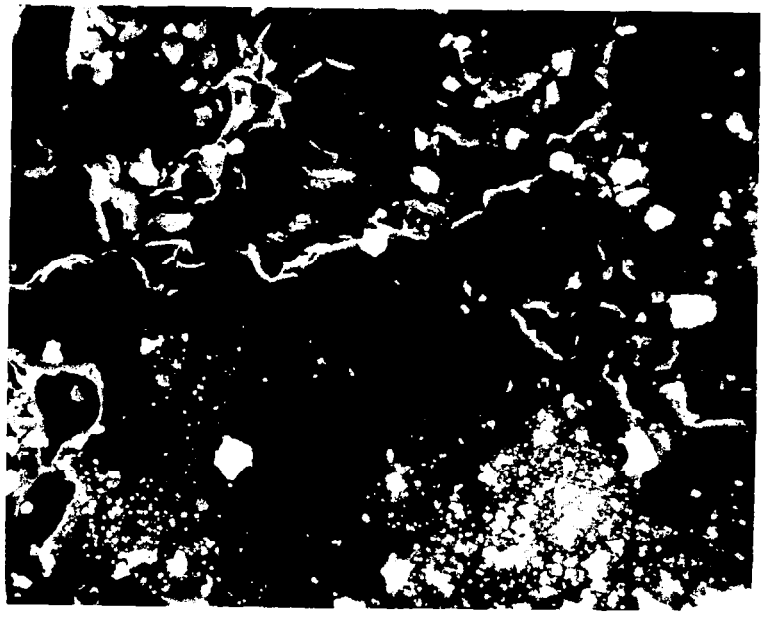

Dark = CaF_2

Light = Ag

Gray = Nichrome

White particles are artifact

(800X)

Figure 31 Decoration color assignment confirmed by EDX analysis.

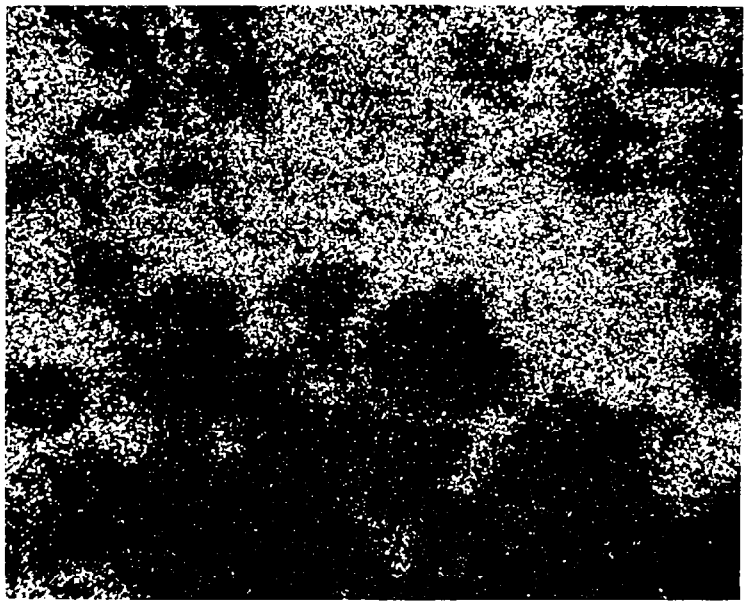

spatial distribution for Ca counts (800X)

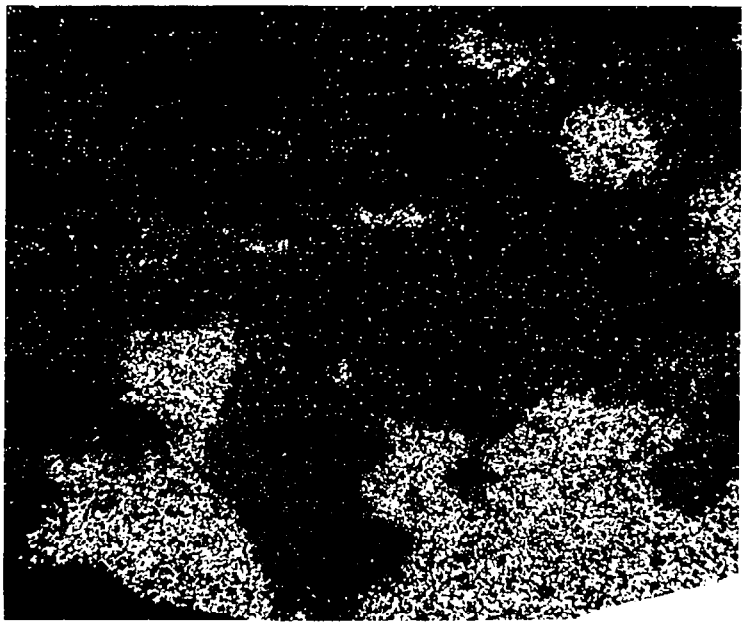

spatial distribution for Ag counts (800X)

Figure 31 Concluded.

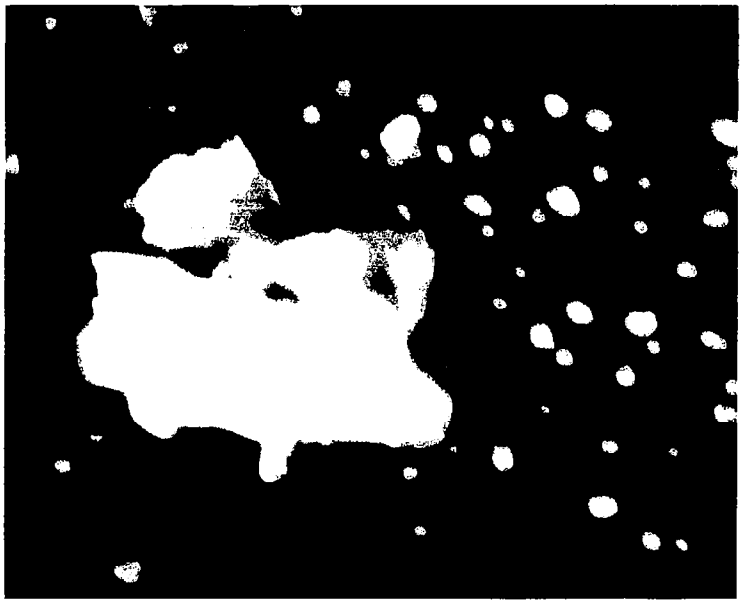

Ag particle showing stipple from oxidation reaction (white particle contains Ca and P as determined by EDX analysis --6000X)

Nichrome particle showing polishing scratches (2400X)

Figure 32 Magnified view of nichrome and decorated Ag particles in polished section.

the most uniform phase distribution and minimum surface porosity. This, coupled with the powder observations, suggested the Batch 13 preparation scheme was close to an optimized one. Table 6 summarizes the observations made concerning the general spraying behavior of these initial trial runs.

3.3.2 Quantitative Microscopy Evaluation

Quantitative microscopy presented one way to evaluate the compositional uniformity of the plasma sprayed coating. By evaluating the distribution of results for the individual 12 point grid placements, the .2"x2" bars, the 2"x2" squares, and for each group of 3 squares devoted to each of two batches, information concerning the scale of uniformity could also be obtained.

Figure 33 shows the dispersion or distribution of counts within the 2x6=12 point grid for the 40 grid placements per .2"x2" bar and summarizes the volume fraction results for each such bar. Ideally, if the compositional distribution was completely uniform on the 56μm x 180μm scale of the 12 point grid, Figure 33 should consist of distribution spikes with all the grid placements giving the following counts:

Material	Specification	x	12 point/ grid	=	Counts
CaF_2	.55	x	12	=	6.6
Nichrome	.25	x	12	=	3.0
Ag	.20	x	12	=	2.4

An individual placement is intended to present a statistically representative measure and hence should tend to show the overall distribution if that distribution is sufficiently random and

TABLE 6

Summary of Observations During Initial Plasma-Spray Trials

Test No.	Material	Gas Flow ARC (CFH)	Gas Flow Powder (CFH)	Power Volts	Power AMPS	Screw Feed (RMP)	Gun Dist. (ins.)	Hopper No.
1	Batch 1	68	21	25	480	100	3-3/4	2
	Ave. 0.016" coat ∿6 passes discoloration, unmelted particles							
2	Batch 2	68	21	25	480	100	3-3/4	2
	Very little feed-powder too fine, tends tc adhere to feed tubes, discoloration							
3	CaF_2 (-325m)	68	21	25	480	140	3-3/4	2
	almost no coat; material will not flow							
4	CaF_2 (-150+325)	68	21	25	480	100		2
	good coat, no discoloration							
5	NiCr 75% CaF_2 25% (-150+325)	68	21	25	480	100	3-1/2	2
	stopped flowing after 4 passes, no brown discoloration							
6	Batch 10	68	21	25	480	100	3-1/2	2
	Good flow for 4 passes then silver melted and plugged port at nozzle of gun; brown discoloration							
7	Batch 10	68	21	25	480	50	2-3/4	1
	Many large agglomerates of unmelted material							
8	Batch 7	68	21	25	520	50	2-3/4	1
	Some large unmelted aggregates							

TABLE 6 Concluded.

Test No.	Material	Gas Flow ARC (CFH)	Gas Flow Powder (CFH)	Power Volts	Power AMPS	Screw Feed (RPM)	Gun Dist. (ins.)	Hopper No.
9	Batch 2	68	21	26	520	50	3	1
	Poor flow, feeding slow, CaF_2 coating nozzle, very little CaF_2 on substrate							
10	Batch 8	68	21	26	560	50	2.0	1
	Fairly good flow conditions; considerable discoloration and unmelted CaF_2 particles.							
11	Batch 12	68	21	26	560	50	4.5	1
	Use frond feed tube; no clogging; appears quite uniform							
12	Batch 13	68	21	26	590	50	4.5	1
	More discoloration than Batch 12 coat; almost clogged feed tube port at nozzle, noticeable amount of melted CaF_2 particles, front feed tube.							
13	Batch 14	68	21	26	595	50	4.5	1
	Front feed tube; less powdering in all feed tubes than Batch 13							

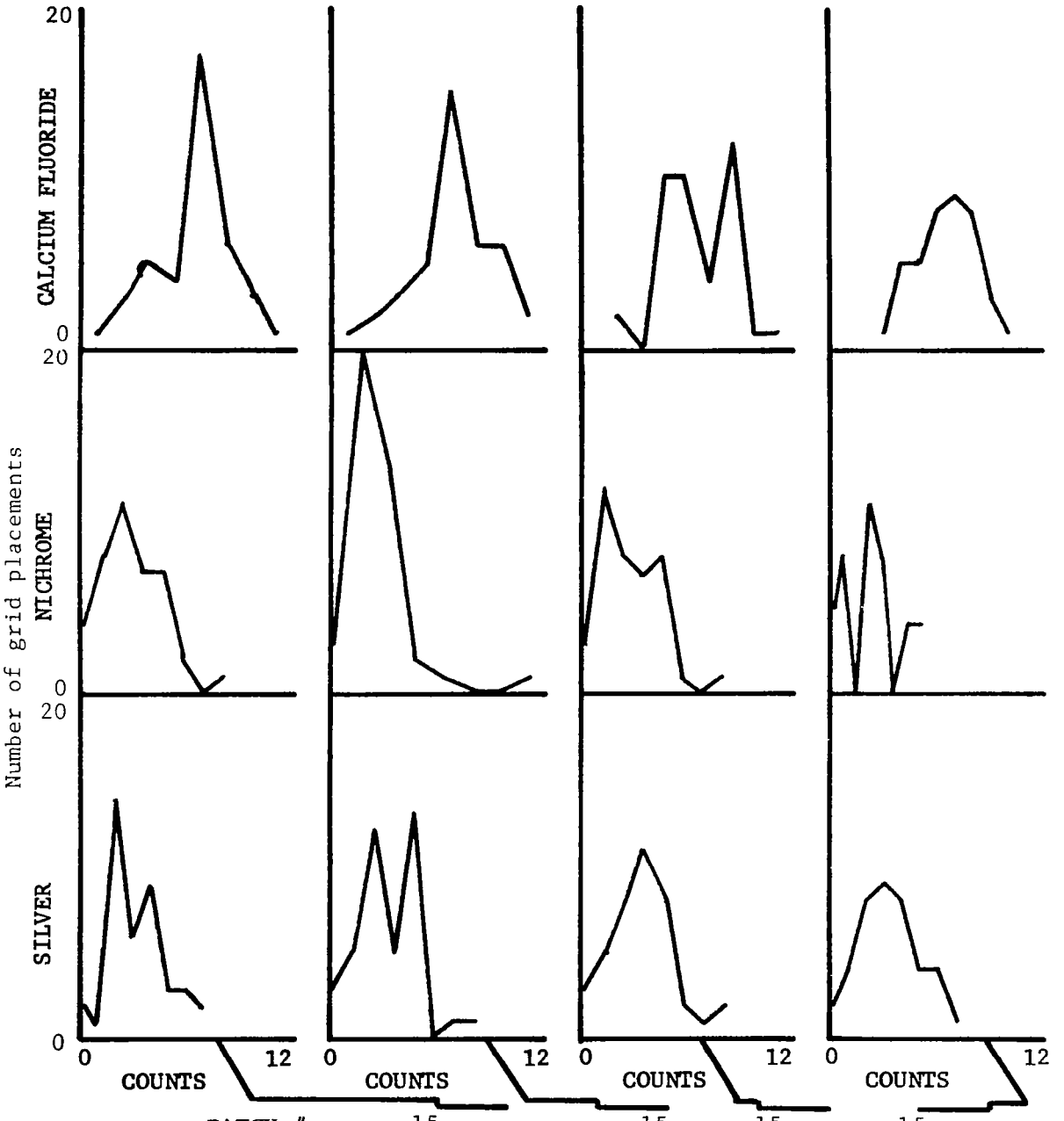

BATCH #	15	15	15	15
SAMPLE #	14A	14C	14E	14G
Vol % CaF_2	51.6±17.5	55.4±18.5	53.8±17.4	54.2±13.9
Vol % Nichrome	21.3±15.2	20.0±15.3	20.2±15.3	18.8±12.3
Vol % Ag	27.1±14.2	24.6±15.4	26.0±16.8	27.1±14.3

Figure 33 Summary of quantitative microscopy results for each .2"x2" bar showing frequency of grid sites have each count level.

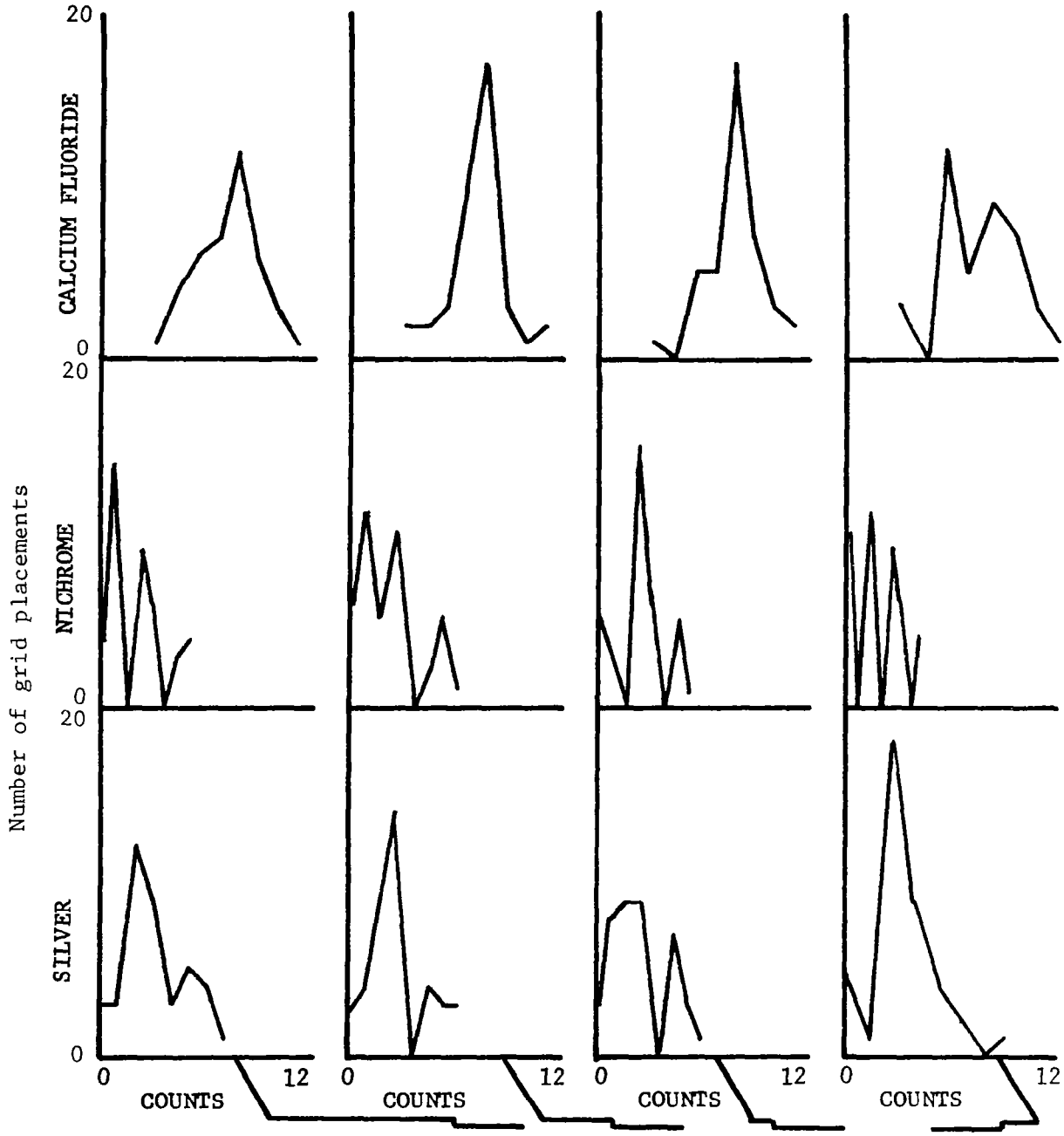

BATCH #	15	15	15	15
SAMPLE #	15A	15C	15E	15G
Vol % CaF_2	57.5±16.6	57.5±15.4	61.9±15.0	61.5±18.5
Vol % Nichrome	17.1±12.2	18.8±14.1	16.9±10.6	13.1±10.8
Vol % Ag	25.4±15.0	23.5±12.9	21.3±12.5	25.4±16.1

Figure 33 Continued.

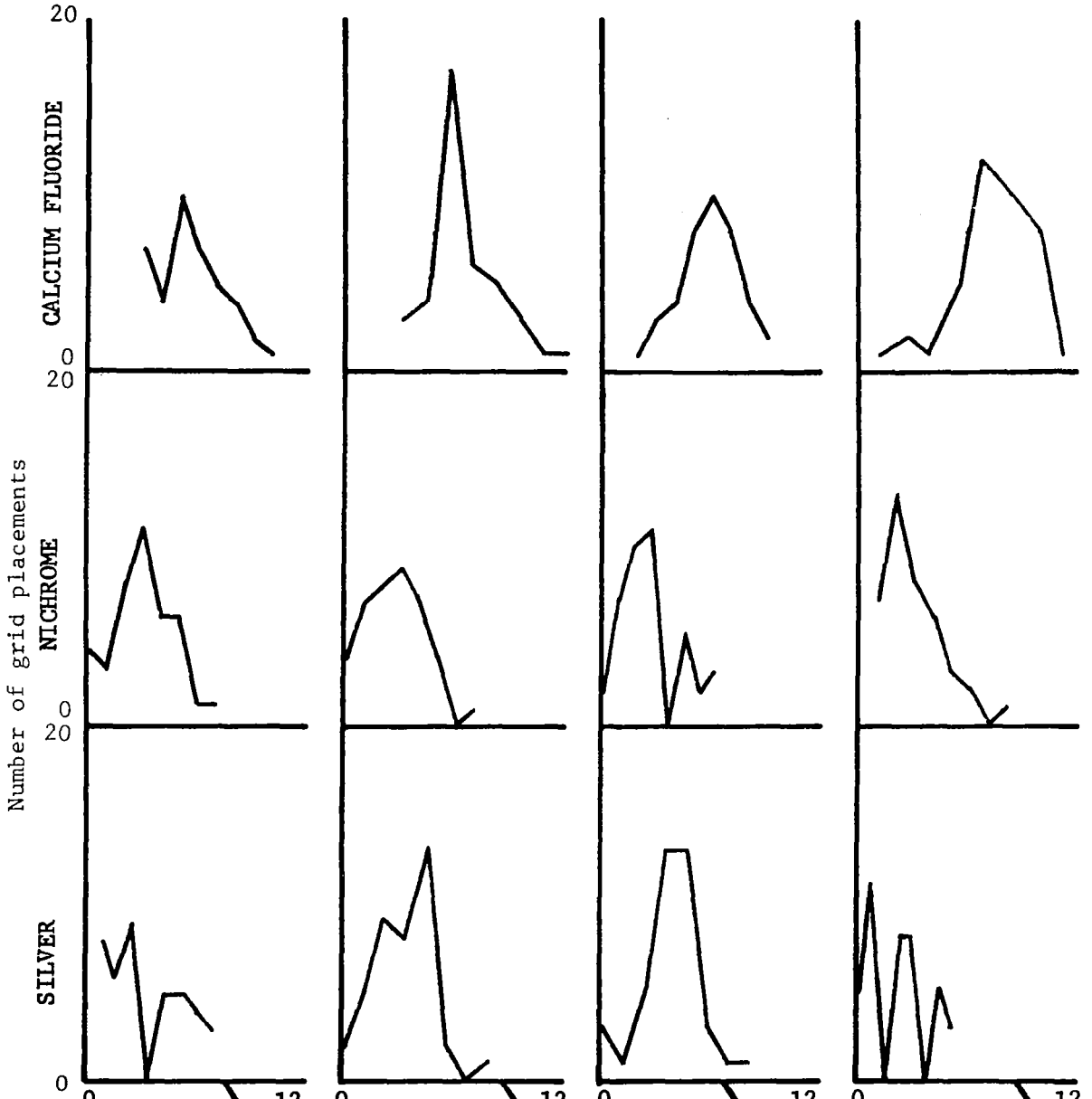

BATCH #	15	15	15	15
SAMPLE #	16A	16C	16E	16G
Vol % CaF_2	46.7±15.7	52.5±17.3	48.5±13.9	58.5±17.7
Vol % Nichrome	24.8±14.1	21.9±13.7	22.5±12.8	24.2±13.5
Vol % Ag	28.5±15.8	25.6±14.3	29.0±14.3	17.9±12.3

Figure 33 Continued.

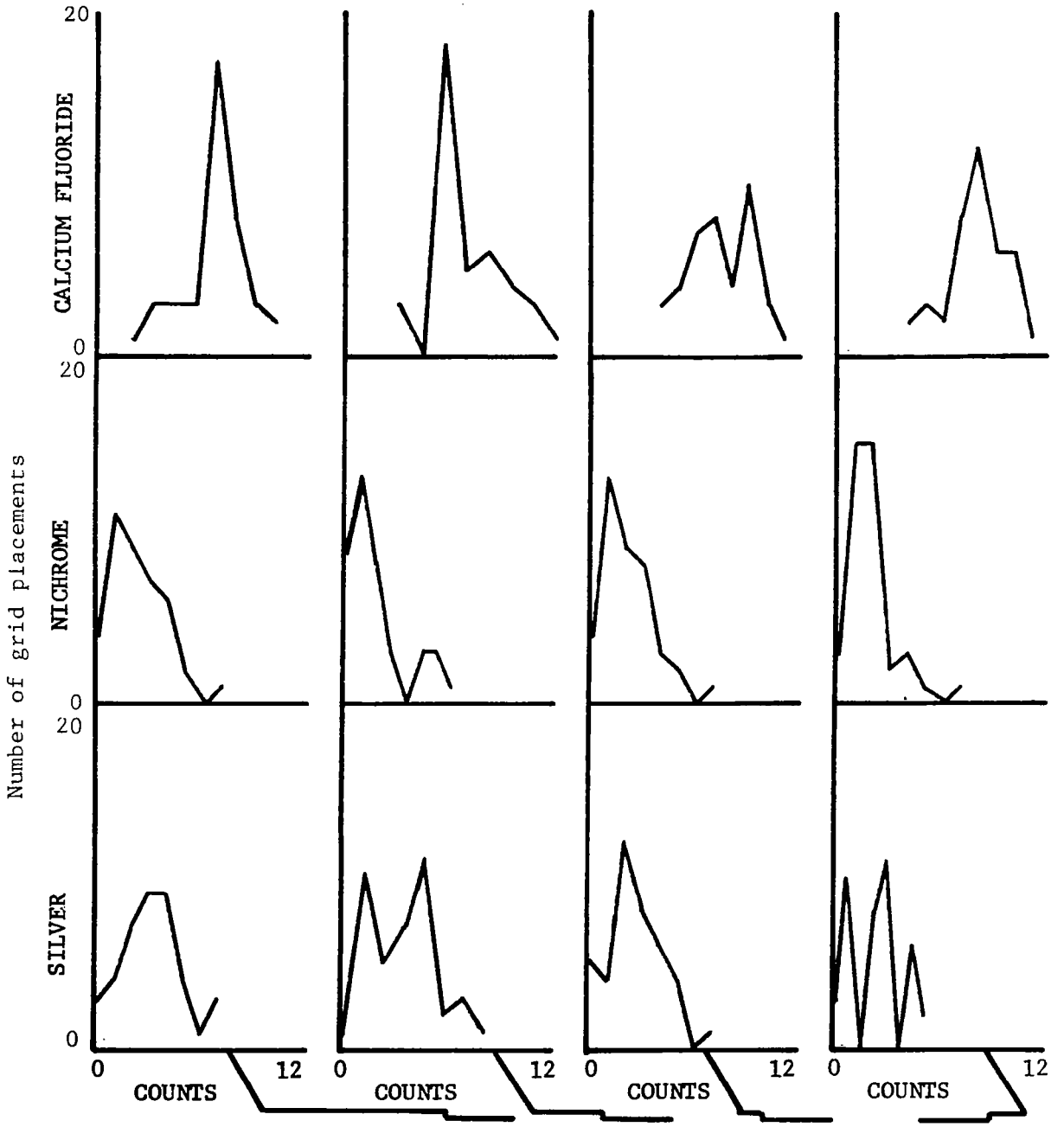

BATCH #	17	17	17	17
SAMPLE #	17A	17C	17E	17G
Vol % CaF_2	54.4±16.2	57.5±18.9	61.0±15.4	65.0±14.1
Vol % Nichrome	19.0±13.2	14.8±13.7	17.5±12.8	15.6±11.5
Vol % Ag	26.7±15.2	27.7±17.5	21.5±13.6	19.4±11.2

Figure 33 Continued.

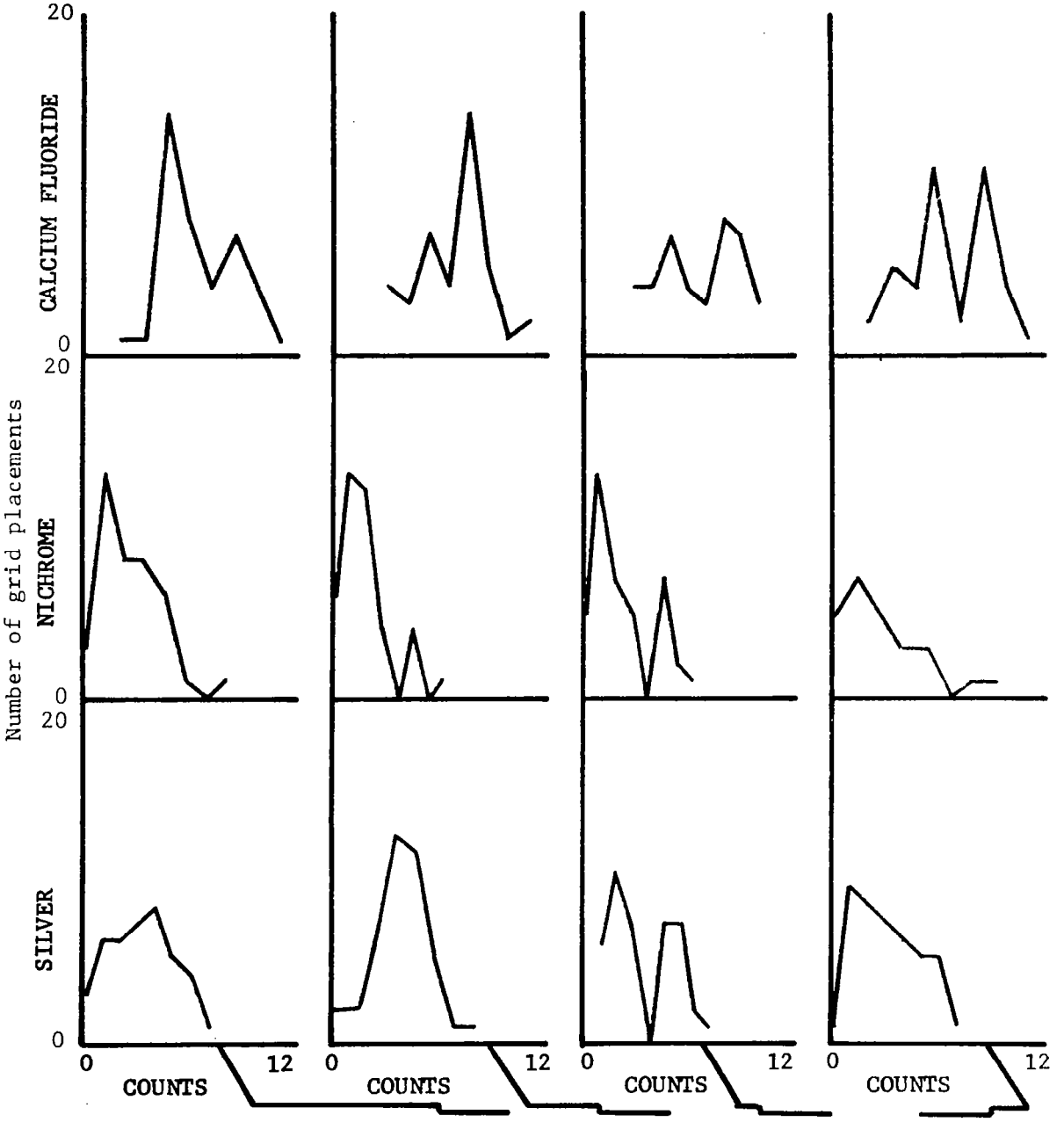

BATCH #	17	17	17	17
SAMPLE #	18A	18C	18E	18G
Vol % CaF_2	$54.4^{+}_{-}17.9$	$55.2^{+}_{-}18.2$	$55.2^{+}_{-}18.4$	$54.0^{+}_{-}20.1$
Vol % Nichrome	$19.2^{+}_{-}14.0$	$14.8^{+}_{-}11.2$	$17.9^{+}_{-}13.3$	$20.8^{+}_{-}16.3$
Vol % Ag	$26.5^{+}_{-}15.5$	$30.0^{+}_{-}15.2$	$26.9^{+}_{-}13.4$	$25.2^{+}_{-}15.0$

Figure 33 Continued.

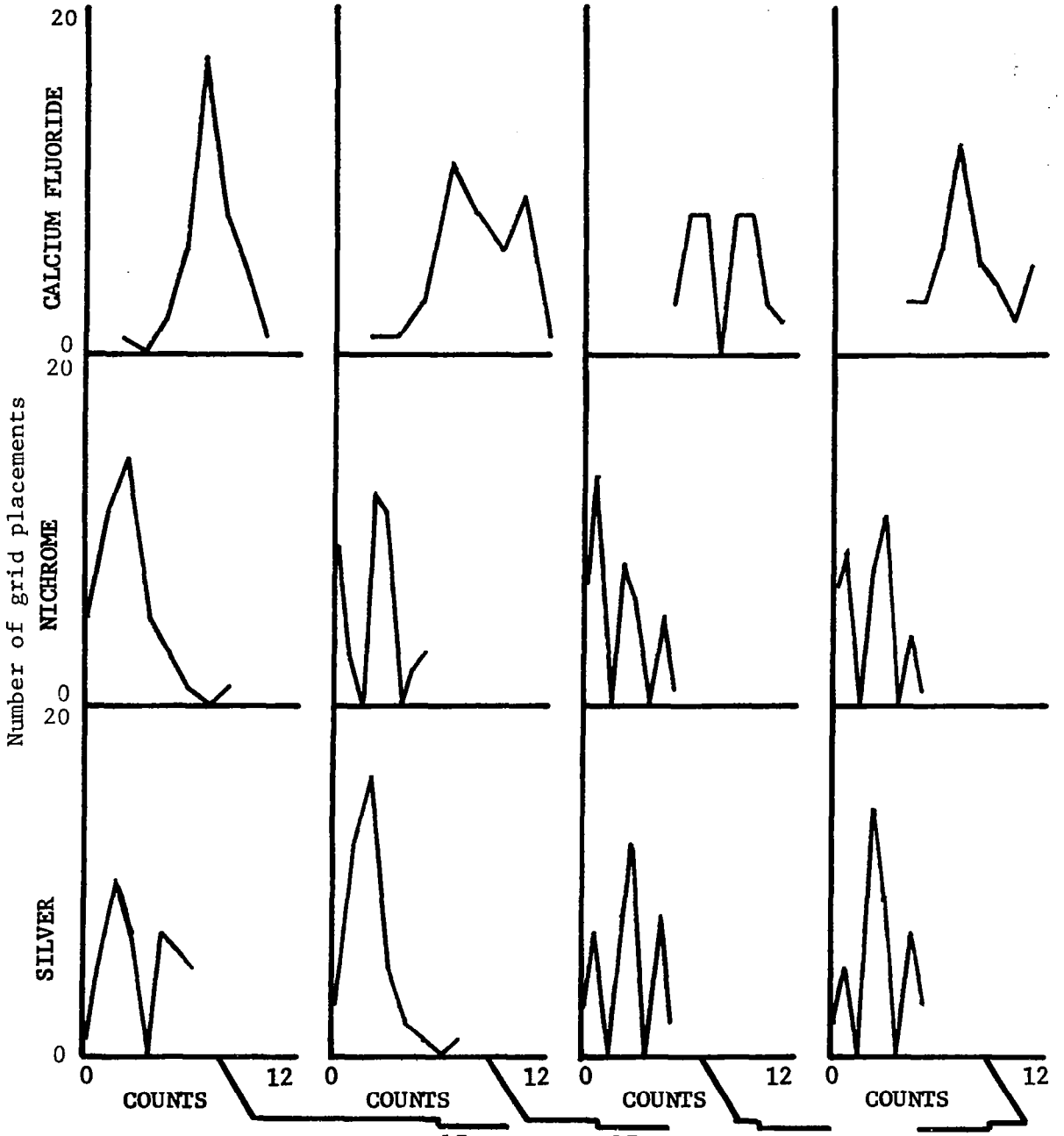

BATCH #	17	17	17	17
SAMPLE #	19A	19C	19E	19G
Vol % CaF_2	56.7 ± 13.9	66.3 ± 17.5	64.0 ± 13.4	62.1 ± 16.7
Vol % Nichrome	16.7 ± 13.3	17.3 ± 12.3	15.0 ± 11.5	16.5 ± 11.4
Vol % Ag	26.7 ± 13.6	16.5 ± 11.2	21.0 ± 11.2	21.5 ± 10.7

Figure 33 Concluded.

uniform itself. However, the grid area examined is only 0.156% of the .2"x2" bar area sprayed and would not be expected to give ideal results since the particle size of the constituents is comparable in some cases to the grid dimensions. The ideal would be more closely approached if the number of grid points and number of grid placements were increased; however, more effort in the counting would also be required and a compromise between accuracy and effort must be made. Although not ideal, Figure 33 does show a strong tendency to center at or near the desired count value with some dispersion evident. This indicates there is a good deal of compositional uniformity on the scale of the grid. The sharp peaks and valleys sometimes present in Figure 33 result from the particular cell size used in computing the number of placements (out of 40) with a given point count. The overall envelope is of primary interest.

The average volume fraction and standard deviation of 40 grid placements for each .2"x2" bar examined are also tabulated in Figure 33 and displayed graphically for each of the two batches in Figures 34 and 35. The required compositional range or specification is also indicated. For Batch 15 the CaF_2 values are all near or within specification while the two metal phases show relatively little variation between bars but are essentially reversed in terms of the specification. (This is what prompted the EDX analysis discussed above). For Batch 17, Sample 18 is within specification for CaF_2 while the other two tend to give higher values. Since the total volume fraction must equal one, the metal values are

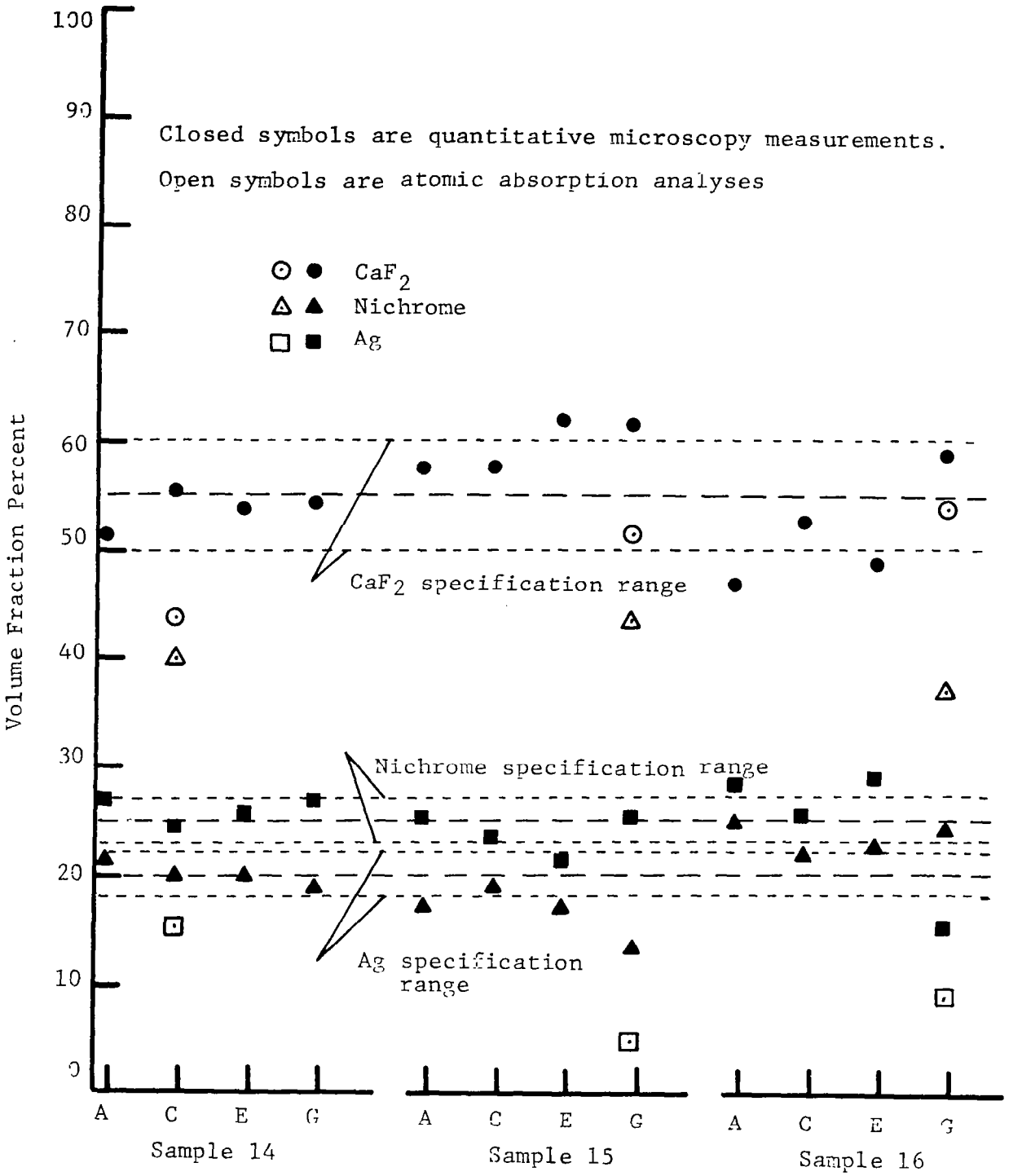

Figure 34 Comparison and distribution of compositional results for quantitative microscopy and atomic absorption using Batch 15 powder.

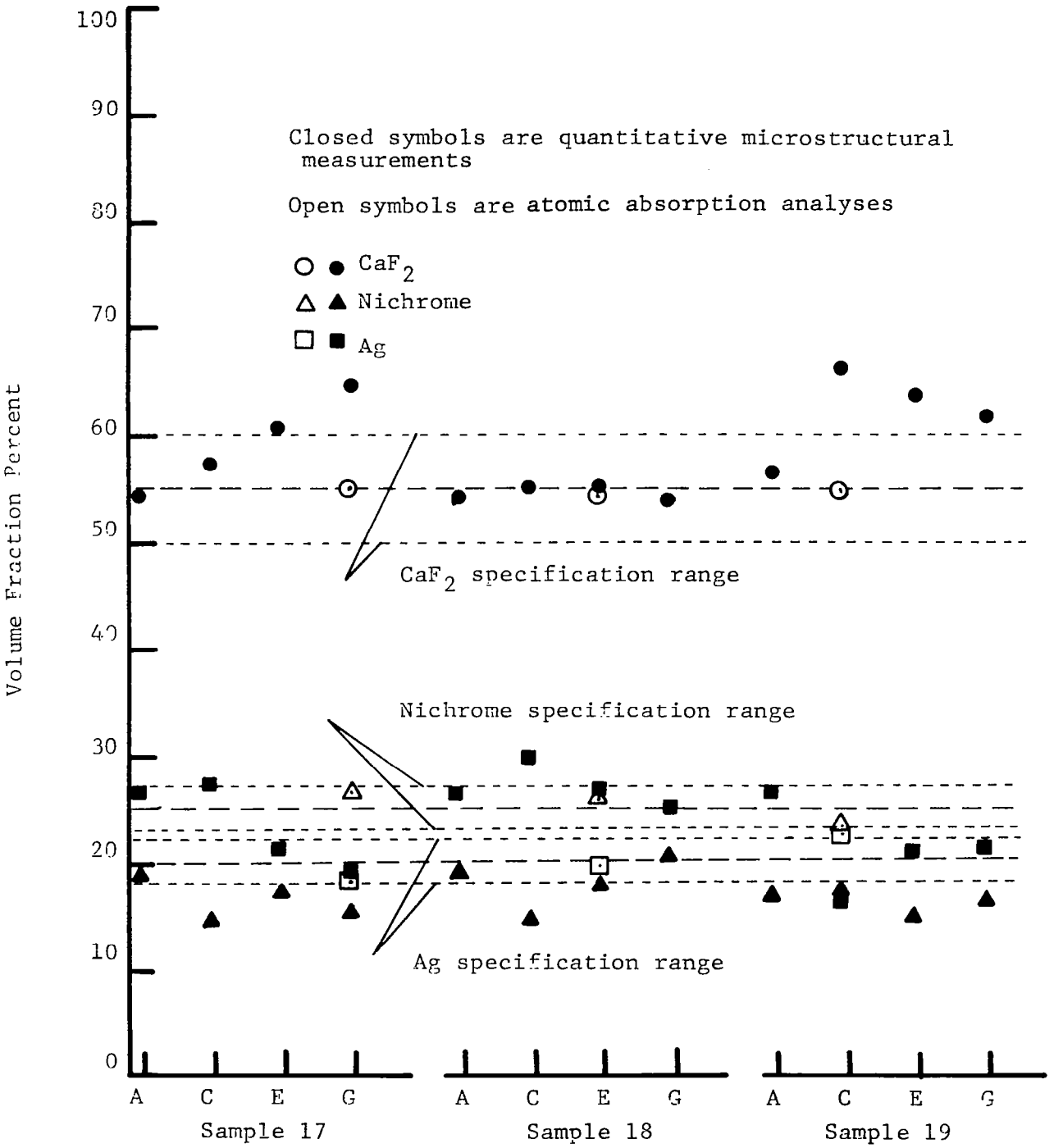

Figure 35 Comparison and distribution of compositional results for quantitative microscopy and atomic absorption using Batch 17 powder.

correspondingly lower and also reversed in terms of the specification (the small level of porosity was ignored in these measurements and is included in the CaF_2 counts). Thus some compositional nonuniformity at the bar and square size level is present, but the general trend is still fairly uniform and what deviations do occur are not large.

The reversal in metal counts may be attributed to a relative loss in nichrome, which causes tha Ag counts to increase in proportion. This could occur if the nichrome is solidifying as it leaves the plasma and might tend to bounce off the coating surface. The CaF_2, of comparable melting point, has a different heat capacity and radiation characteristics and so may remain "solf" until impact. The Ag was confirmed by observations on glass slides to be molten and splatter upon impact, probably acting somewhat as a "glue" for the other particles as it froze. The reversal of metal quantities may be remedied by increasing the nichrome level in the starting powder.

Table 7 presents the averages for each 2"x2" area and for each of the two batches sprayed. At this level there is still variation in composition, but each square (except #19) is within specification for CaF_2. The range in Ag for samples 15, 17, and 19 is greater than specified, but the nichrome range is within the desired limits. The agreement for each material between the two overall batches is good.

Table 7

Sample and Batch Averages for
Quantitative Microscopy Measurements

BATCH SAMPLE	15 14	15 15	15 16	BATCH AVERAGE
Vol % Ca F_2	53.8±1.6	59.6±2.4	51.6±5.2	55.0±4.7
Vol % Nichrome	20.1±1.0	16.5±2.4	23.4±1.4	20.0±3.3
Vol % Ag	26.2±1.2	23.9±2.0	25.3±5.1	25.1±3.1

BATCH SAMPLE	17 17	17 18	17 19	BATCH AVERAGE
Vol % CaF_2	59.5±4.6	54.7± .6	62.3±4.1	58.8±4.6
Vol % Nichrome	16.7±1.9	18.2±2.5	16.4±1.0	17.1±1.9
Vol % Ag	23.8±4.0	27.2±2.0	21.4±4.2	24.1±4.0

Quantitative microscopy has indicated a strong tendency to compositional uniformity on a microstructural scale, some variation at the size level of sample bars and 2"x2" squares, but overall good agreement between the two batches. Making more point counts and increasing the amount of nichrome in the starting powder should improve the compositional uniformity even more than already observed.

3.3.3. Atomic Absorption Determinations

Table 8 presents the results obtained on selected bar samples and a mixture of Batch 15 and 17 powder. Since only analyses for Ag and Ca were performed, the CaF_2 level was calculated from the Ca and the nichrome amount was obtained by difference. These results are displayed in Figures 34 and 35 for comparison to the quantitative microscopy results.

In general the agreement between the two measurements is poor. Even the results for the powder mixture, where minimal loss of material is expected, do not agree with the nominal starting batch composition. For the Batch 15 samples the Ag measurement is much lower than either the desired or the quantitative microscopy measurement amounts. This raises the corresponding level for nichrome. On the other hand, Batch 17 results suggest these coatings are exactly within specification: no metal quantity reversal is seen although agreement with microscopy measurements for CaF_2 is poor. Personnel at the commercial

Table 8

Results of Wet Chemical Analyses

Sample No.	CaF_2*		Nichrome**		Ag	
	Vol %	Wt %	Vol %	Wt %	Vol %	Wt %
1-14C	43.7	21.6	40.1	53.3	15.4	25.1
2-15G	51.4	28.2	43.6	62.9	4.9	8.9
3-16G	53.9	29.8	37.1	53.9	8.9	16.3
4-17G	55.0	29.6	26.6	37.7	18.4	32.7
5-18E	54.3	29.0	26.4	37.0	19.3	34.0
6-19C	54.7	29.0	23.0	32.0	22.2	39.0
7***	44.2	22.0	41.0	53.6	14.8	24.4

* Obtained from measurement of Ca wt %

** Obtained by substracting the measured CaF_2 and Ag values from 100

*** Mixture of Batch 15 amd 17 powders.

laboratory could not explain this discrepancy but did express a willingness to try to resolve the differences between the two measurements. In light of the low Ag measured in Batch 15 and poor agreement with the as-supplied powder composition, it appears these atomic absorption measurements can not reliably be used to check or confirm the quantitative microscopy results. Additional work is needed to resolve the observed differences and determine a good, simple technique for quality control measurements in a vendor organization.

3.4 Adhesive Strength Results

The adhesive strength results are shown in Table 9 before and after a 20 hour, 649°C heat treatment in air. The strength increased approximately 40% after the heat treatment. One sample was erroneously low and its value was discarded. Examination of the failure surface for this discarded sample showed fibrous strands that looked like cotton. These were attributed to bonding adhesive which had impregnated the coating during setting and joining the two halves of the test-sandwich. This was pulled like taffy during the test but also provided a relatively weaker bond in this form. Photographs of the failure surfaces made through an optical microscope did not show sufficient depth of field to be useful and so were not included in this report.

4.0 RECOMMENDATIONS FOR FUTURE WORK

The results obtained to date essentially meet the goals established at the outset of the program. However, some areas need additional refinement, the successes already obtained suggest

Table 9.

Adhesive Strength Results

As-plasma-sprayed strengths (psi):	740
	190*
	600
	1135
	734
	965
Avg.:	835
Strength after 20 hours, 649°C heat treatment in air (psi):	1120
	1210
	1170
Avg.:	1167

* Value considered invalid

more areas where they could be applied, and it is known several new areas exist of strong and common interest to both NASA and IITRI personnel. This section presents some of these.

1. Develop an automated plasma spraying set-up. A shaper available at IITRI should provide a good start for a laboratory scale machine. This is considered to be a relatively small effort to optimize the equipment already on hand.

2. Expand the quantitative microstructural analysis technique as to decoration methods, polishing procedure, possible use of automatic counting facilities (i.e., Quantimet 720 image analyzing computer), and development of a scheme suitable for use as a quality control or confirmatory index in a vendor's shop. Additional correlation of this measurement to other techniques, such as wet chemical, atomic absorption, EDX-SEM distribution display, and x-ray diffraction would also increase general confidence in the measured results. Such effort is especially important as the number and type of phases considered, e.g., porosity and glass, cobalt alloys, etc., are increased.

3. Examine past NASA and/or vendor coatings using quantitative microscopy for their compositional distribution and level; and then correlate these results with measured friction and wear behavior. This will provide an important baseline to compare the additional processing improvements and compositional changes made in the future.

4. Examine the mechanical adhesion strength with and without several different prime coatings, such as nichrome and nickle-aluminide coatings. Standard ASTM methods would be appropriate here. It may also be of interest to consider other mechanical property tests, such as a bend test of a coated sheet monitored using gages, deflectometer, and/or acoustic emmission. Another possibility would be torsional or Rumanian shear evaluations of the coating-substrate bond.

5. Examine the processing of other coating compositions containing Co or other alloy powders and/or containing the low Na content glass for improved oxidation resistance.[4]

6. Examine coating performance under cyclic thermal loads such as water bath, oil bath, fluidized-bed, or torch-air quench systems. Both up-quenches and down-quenches (possibly to liquid N_2) would be appropriate considering the potential high temperature and cyrogenic temperature range of application for these coatings.

7. Develop the techniques needed to produce up to 20 lbs. of high purity, low Na content glass for use as an oxidation inhibitor in the coatings. IITRI has extensive experience in glass-ceramics, and property evaluation of glass (such as temperature-shear characteristics). One or more of these could be used as a quality control test for the glass compositional uniformity.

8. Basic study of the oxidation of these coatings and/or their oxidation protection using DTA, TGA, and x-ray techniques as a function of atmosphere and temperature. This would be especially informative when coupled with microstructural examination at both the optical and electron microscope levels.

9. Examine possible use of other composite powder preparation techniques, such as spray drying. This is important if large quantities of powder must be produced.

Any of the above would be an interesting and exciting contribution to the area of solid, high-temperature lubricants.

REFERENCES

1. H. E. Sliney, "Preliminary Evaluation of Greases to 600°F and Solid Lubricants to 1500°F in Ball Bearings," A.S.L.E. Trans., 11, 330-37 (1968)

2. H. E. Sliney, "An Investigation of Oxidation-Resistant Solid Lubricant Materials," Ibid., 15, 177-83, (1972).

3. H. E. Sliney, "Plasma-Sprayed Metal-Glass and Metal-Glass Fluoride Coatings for Lubrication to 900°C," Ibid., 17 182-89, (1974).

4. H. E. Sliney, "Bearing Material," U.S. Patent No. 3,953,343, granted April 27, 1976.

5. Science of Ceramic Processing Before Firing, 10th University Conference on Ceramic Science, January, 1975.

6. A.L. Wertheimer and W. L. Wilcox. "Light Scattering Measurements of Particle Distributions, "Applied Optics, 15 1616-20 (1976).

7. E. L. Weiss and H. N. Frock, "Rapid Analysis of Particle Size Distributions by Laser Light Scattering," Powder Technology, 14 287-293 (1976).

8. H. L. Rechter, "Development of Bonding Methods and Materials for Electrical Strain Gages,: Summary Report No. 2, ARF Project No. 6042-5, 1960.

9. G. Y. Onoda and E. Ong, "Research on Binders in Ceramic Processing," IITRI Project No. G8039, Report #6, 1972.

10. F. N. Rhines, "Origins of Quantitative Metallography" Met. Soc. Conf., 27, 417-34 (1963).

11. Quantitative Microscopy, R. T. Dehoff and F. N. Rhines, eds, McGraw-Hill, New York, 1968.

12. H. F. Fischmeister, "Applications of Quantitative Microscopy in Materials Engineering," J. Microscopy, 95 (pt. 1 119-43 (1972).

13. Fourth International Congress for Stereology, Proceedings Ed. by E. E. Underwood, et.al., NBS Spec. Publ. 431, 1976.

14. C. Fisher, "The New Quantimet 720," The Microscope, 19 1-4 (1971).

APPENDIX - PREPARATION OF COMPOSITE PLASMA-SPRAY POWDER MIXES

Batch Nos. 15-20 were all prepared in the same manner. The basic composition of the mix consisted of the following powders.

	% by wt.	100 gm batch, gm
Nichrome	35	38.5
Ag	35	38.5
CaF_2	30	33.0

Monoaluminum Phosphate binder*
(MAP) in the form of a 20 vol.% solution gave a solid content of 3.8 wt.% added to the above.

For a 110gm batch, the total wt. including dried MAP = 114.2gm.

Particle size of the powders

Nichrome**	– 150+325 mesh	38.5g
Ag**	– 200+325 mesh	38.5g
CaF_2***	– 5μm	19.3g (58% of 33g)
CaF_2**	– 150+325 mesh	13.7g (42% of 33g) plus an extra amount to compensate for cured material lost during final sieving through -325 mesh

*Mobil Chemical Co.
Richmond, VA
**Cerac, Inc.
Milwaukee, WI
***Fisher Co.
Chemical Mfg, Div.
Fair Lawn, NJ

The following procedure was used to prepare the mixes for a 110gm batch.

Step 1.

Ball Mill Nichrome 38.5g
Ag 38.5g
CaF_2 19.3g
with 1/2" diameter nylon balls for 1 1/2 hours.

Step 2.

Add 27cc of a 20 vol.% MAP solution to the mix in an evaporating dish, heat, constantly stirring to a damp dryness. Sieve the damp/dry material through a 20 mesh screen.

Step 3.

Dry in oven at 110-115°C overnight.
Sieve through a 70 mesh screen.

Step 4.

Cure at 400 - 450°C for 1 1/2 hours.
Screen through -70+325 mesh.

Step 5.

To the -70+325 mesh material add CaF_2 (-150+325 mesh size). The amount to add is 13.7g + an amount equal to the weight of material lost through the 325 mesh.

Step 6.

Ball mill lightly without any mixing balls for 10 minutes.

1. Report No.	2. Government Accession No.	3. Recipient's Catalog No.
NASA CR-3163		

4. Title and Subtitle	5. Report Date
PROGRAM FOR PLASMA-SPRAYED SELF-LUBRICATING COATINGS	July 1979
	6. Performing Organization Code
7. Author(s)	8. Performing Organization Report No.
G. C. Walther	D6146
	10. Work Unit No.
9. Performing Organization Name and Address	
IIT Research Institute 10 W. 35th St. Chicago, Illinois 60616	11. Contract or Grant No. NAS 3-20827
	13. Type of Report and Period Covered
12. Sponsoring Agency Name and Address	Contractor Report
National Aeronautics and Space Administration Washington, D.C. 20546	14. Sponsoring Agency Code

15. Supplementary Notes

Final report. Project Manager, Harold E. Sliney, Fluid System Components Division, NASA Lewis Research Center, Cleveland, Ohio 44135.

16. Abstract

A program was conducted to establish powder processing and plasma spray parameters to reproducibly achieve a well bonded, low porosity coating of NASA LUBE PS106 which has the nominal composition by weight percent of 35 silver, 35 nichrome, and 30 calcium fluoride. A method for preparing composite powders of the three coating components was developed and a procedure that can be used in applying uniform coatings of the composite powders was demonstrated. Composite powders were prepared by adjusting particle sizes of the components and employing a small amount of monoaluminum phosphate as an inorganic binder. Quantitative microscopy (image analysis) was found to be a convenient method of characterizing the composition of the multiphase plasma-sprayed coatings. Area percentages and distribution of the components were readily obtained by this method. The adhesive strength of the coating to a nickel-chromium alloy substrate was increased by about 40 percent by a heat treatment of 20 hours at 650° C.

17. Key Words (Suggested by Author(s))	18. Distribution Statement
Solid lubricants; Self-lubricating composite; Wide-temperature-spectrum lubricant; Plasma-sprayed lubricant; Bearing material; Lubricant coating; Inorganic composite	Unclassified - unlimited STAR Category 27

19. Security Classif. (of this report)	20. Security Classif. (of this page)	21. No. of Pages	22. Price*
Unclassified	Unclassified	79	A05

* For sale by the National Technical Information Service, Springfield, Virginia 22161

NASA-Langley, 1979